

Machine Learning as a “Catalyst” for Advancements in Carbon Nanotube Research

Guohai Chen ^{1,*} and Dai-Ming Tang ^{2,3,*}

¹ Nano Carbon Device Research Center, National Institute of Advanced Industrial Science and Technology (AIST), Tsukuba Central 5, 1-1-1 Higashi, Tsukuba, Ibaraki 305-8565, Japan

² Research Center for Materials Nanoarchitectonics (MANA), National Institute for Materials Science (NIMS), Tsukuba, 305-0044, Japan

³ Institute of Pure and Applied Sciences, University of Tsukuba (Collaborative University), Tsukuba, 305-8571 Japan

* Correspondence: guohai-chen@aist.go.jp (G.C.), TANG.Daiming@nims.go.jp (D.T.)

Abstract: The synthesis, characterization, and application of carbon nanotubes (CNTs) have long posed significant challenges due to the inherent multiple complexity nature involved in their production, processing, and analysis. Recent advancements in machine learning (ML) have provided researchers with novel and powerful tools to address these challenges. This review explores the role of ML in the field of CNT research, focusing on how ML has enhanced CNT research by: (1) revolutionizing CNT synthesis through the optimization of complex multivariable systems, enabling autonomous systems, and reducing reliance on conventional trial-and-error approaches; (2) improving the accuracy and efficiency of CNT characterizations; and (3) accelerating the development of CNT applications across several fields such as electronics, composites, and biomedical fields. The review concludes by offering perspectives on the future potential of integrating ML further into CNT research, highlighting its role in driving the field forward.

Keywords: carbon nanotube; machine learning; data-driven; chemical vapor deposition; synthesis; characterization; application

1. Introduction

1.1. Machine Learning

Recently, machine learning (ML), a new paradigm, has demonstrated great potential as a tool for materials research [1-3]. ML is a subset of artificial intelligence (AI) concerned with the development and study of algorithms and statistical models that can learn from data and generalize to unseen data and thus perform tasks without explicit instructions. Instead of following predetermined instructions, ML systems learn from data to recognize patterns, make decisions, and improve their performance over time [4-10].

ML has shown a wide range of applications across various domains, such as materials research, healthcare, finance, retail, autonomous vehicles, language processing, etc. Specifically, in the field of materials science, ML has been applied to various aspects and demonstrated great success [11]. Some of them are briefly discussed here (Figure 1).

(1) Materials discovery. ML has significantly accelerated the discovery of new materials, showing great advantages compared with traditional approaches which has been slow and labor-intensive, involving extensive experimentation and trial-and-error processes [12, 13]. ML offers a data-driven alternative, enabling the prediction of new materials with desired properties. With the assistance of ML, high-throughput screening allows thousands or even millions of potential compounds to be evaluated computationally using trained ML models before selecting a few candidates for real experimental testing.

Citation: To be added by editorial staff during production.

Academic Editor: Firstname Last-name

Received: date

Revised: date

Accepted: date

Published: date



Copyright: © 2024 by the authors. Submitted for possible open access publication under the terms and conditions of the Creative Commons Attribution (CC BY) license (<https://creativecommons.org/licenses/by/4.0/>).

Additionally, inverse design becomes feasible, where researchers begin with the desired material properties and use ML algorithms to identify the structures or compositions that can achieve those properties. For instances, Rao et al. used an iterative scheme that combines ML, density functional theory, experiments, and thermodynamic calculation to find two new invar alloys with extremely low thermal expansion out of millions of candidates. The alloys are both compositionally complex, high entropy materials, thus demonstrating the power of this approach for materials discovery [14].

(2) Process optimization. ML is also revolutionizing the optimization of manufacturing/synthesizing processes in materials science. These processes often involve multiple complex variables, such as temperature, pressure, gas, and time, which must be carefully controlled to achieve optimal results, however, the variable space is far too vast to exhaustively explore experimentally. ML enables more efficient optimization by analyzing complex datasets and identifying the most critical parameters. For example, in the field of chemical vapor deposition (CVD) synthesis of single-walled carbon nanotubes (SWCNTs), Rao et al. utilized ML to find optimal synthesis conditions within one hundred experiments for selectively growing SWCNTs within a narrow diameter range [15]. Lin et al. predicted growth conditions toward addressing the synthetic trade-off between crystallinity and growth efficiency of SWCNT forests by training a ML regression model and validated in less than 50 tests [16]. ML significantly advanced the process optimization, especially for complex multivariable systems.

(3) Materials characterization. ML is being integrated into the characterization of materials, where it can reveal hidden patterns in complex datasets and automate the analysis of experimental results [17, 18]. ML, particularly deep learning techniques such as convolutional neural networks, is used to analyze microscopy images to automatically classify microstructural features in the images, such as defects, phase boundaries, grain structures, and particles. etc. ML is also used to analyze data from various spectroscopic techniques, including Raman [19, 20], infrared [21, 22], and X-ray photoelectron spectroscopy (XPS) [23-26]. ML can deconvolute complex spectra, identify chemical species, and quantify material composition. For example, Dee et al. performed quantitative analysis of catalyst nanoparticles for CNT synthesis using high-resolution, high-rate video capture of environmental transmission electron microscopy experimentation coupled with automated image processing, involving computer vision ML algorithms and convolutional neural networks [27]. The automation using ML accelerates the analysis process and provides more consistent and objective results [28].

(4) Property Prediction. Predicting the properties of materials, such as mechanical, thermal, electronic, and optical properties, based on their composition and structure is one of key applications of ML in materials science. This is particularly useful for materials where experimental property measurement is challenging or time-consuming. For instance, Hajilounezhad et al. predicted mechanical properties, including stiffness and buckling properties of CNT forests, using an image-based ML classifier model, showing an accuracy of >91% [29].

(5) Design of experiments (DoE). ML is greatly enhancing the DoE by enabling more efficient exploration of the experimental parameter space. Traditionally, DoE involves systematically varying a few parameters to identify optimal conditions. However, this approach can be limited when dealing with high-dimensional spaces with many variables. Leveraging ML analysis alongside the DoE approach allows for using limited resources, particularly time, more efficiently and increases the likelihood of achieving a true optimum. For example, Cao et al. successfully optimized the materials and devices of organic photovoltaics via the combination of ML and DoE [30].

In summary, ML is profoundly impacting various aspects of materials science, from the discovery of new materials and the optimization of manufacturing/synthesizing processes to the prediction of material properties and the automation of materials characterization. These advancements are accelerating the pace of innovation, reducing the time and cost associated with materials development, and enabling the design of materials

with unprecedented precision and desired functionality. As ML techniques continue to evolve, their integration into materials science will likely become even more pervasive, driving further breakthroughs and opening up new possibilities in this dynamic field.

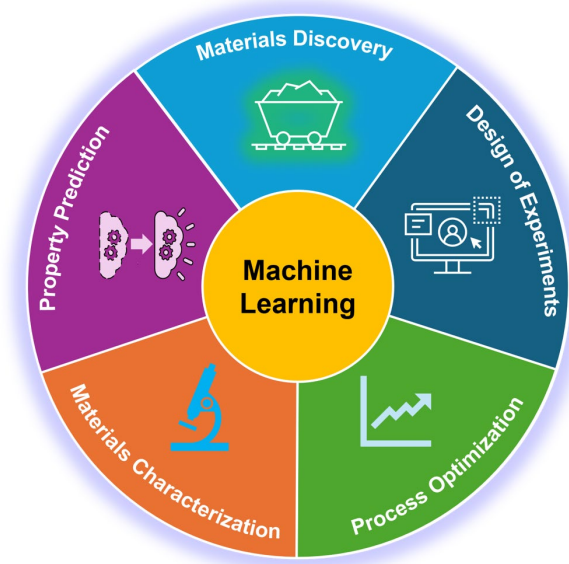


Figure 1. Machine learning-assisted materials research in various aspects.

1.2. Carbon Nanotubes

Carbon nanotubes (CNTs) represent a sub-realm of materials science and a cross-discipline field that intersects with chemistry and applied physics. CNTs, a specific allotrope of carbon, are cylindrical structures characterized by diameters in the nanometer range and lengths that can span from nanometers to centimeters. Due to their unique one-directional structures, CNTs exhibit exceptional mechanical, electrical, and thermal properties. Specifically, CNTs possess remarkable tensile strength, excellent electrical conductivity, and superior thermal stability. These qualities make CNTs highly promising for a broad spectrum of applications, including electronics, composites, energy storage, and biomedical engineering. In electronics, CNTs are being explored for their potential in field-effect transistors [31, 32], touch panels [33], and field emitters [34, 35] due to their high conductivity and electron mobility. In energy-related applications, CNTs have demonstrated significant promise in supercapacitors [36, 37], hydrogen storage [38, 39], and lithium-ion batteries [40, 41], where their high surface area and electrical properties improve energy density and charge capacity. In the biomedical field, CNTs are being researched for biosensors/bioelectrodes [42, 43] and drug delivery systems [44], taking advantage of their biocompatibility and structural versatility. Additionally, through-silicon-via interposers [45] and CNT-based dry adhesives [46, 47] are being developed for use in advanced manufacturing and semiconductor technologies.

ML has also proven to be highly beneficial across numerous facets of research and development of CNTs, given the nature of the involvement of a vast array of intricate and multifaceted parameters. As a special one-dimensional molecule with a unique tubular structure, controlling the atomic structures, characterizing the distinct chirality, and establishing the relationship between properties, structures and device performance for CNTs are significantly more challenging. The complexity of CNT synthesis, which includes factors such as catalyst composition/structure, temperature, synthesis ambient, carbon feedstock, growth enhancers, and reaction conditions, presents additional significant challenges. ML can address them by identifying patterns and optimizing processes that would be difficult or time-consuming to achieve through traditional experimentation methods. Moreover, ML has facilitated the interpretation of large datasets from CNT

characterizations, enabling researchers to uncover subtle correlations and predict properties with greater accuracy. This ability to manage and analyze complex data sets has proven indispensable in advancing CNT applications, where precise control over structural properties can lead to innovations in fields ranging from electronics to materials science. Consequently, the role of ML plays in CNT research continues to grow, offering the potential to unlock new possibilities and drive further progress in this cutting-edge area of nanotechnology.

This short review briefly highlights the significant contributions of the ML approach to CNT synthesis, characterizations, and applications, demonstrating how ML has substantially advanced the CNT research. Finally, the review concludes with a perspective, offering insights into potential future developments and directions for deeper integrating ML into CNT research to drive the field forward.

2. Machine Learning-Assisted CNT Synthesis

Synthesis of CNTs involves complex multivariable parameters. A typical CVD synthesis process of CNTs includes catalyst preparation, catalyst nanoparticle formation, and CNT growth, targeting the desired CNT structural properties (Figure 2a) [48]. As shown in Figure 2b, all these processes are highly sensitive to a vast range of parameters including, but not limited to, catalyst type (composition: commonly used elements such as Fe, Co, Ni or their alloys; structure: single-layer or multi-layer; preparation method: sputtering, evaporation, casting, spin coating, etc.), temperature, pressure, carbon feedstock (type and concentration), growth enhancer (type and concentration), ambient (carrier gas type and concentration), time, etc. [49–51]. These parameters must be meticulously controlled to achieve CNTs with desired structural properties [52], typically including length [53], crystallinity [54], diameter [55], wall number [56], surface area [57], alignment [58], density [59], etc.. Traditionally, optimizing these parameters has relied heavily on trial-and-error approaches, which are time-consuming, labor-intensive, and may not fully capture the complex interactions between these variables. ML has emerged as a powerful tool to address these challenges, offering data-driven strategies for efficiently optimizing CNT synthesis parameters and even enabling the development of autonomous synthesis systems.

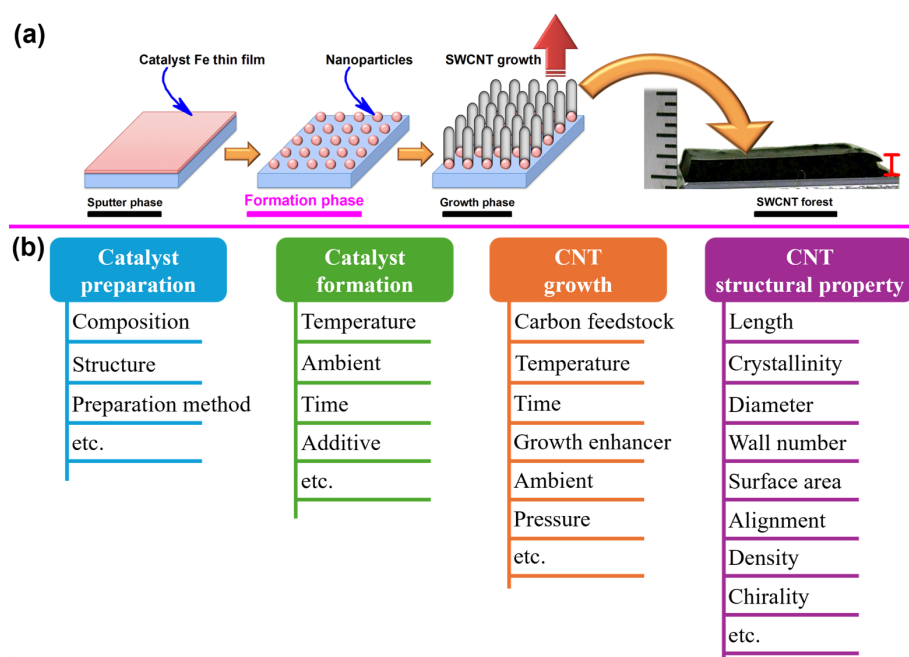


Figure 2. (a) A typical CNT CVD synthesis process. Reprinted with permission from Reference [48]. (b) Complex multivariable parameters in CNT synthesis process.

2.1. Data-Driven Optimization of CNT Synthesis

Data-driven optimization generally refers to the use of ML algorithms to analyze large datasets generated from CNT synthesis experiments and focuses on optimizing the multitude of variables involved in the production process. By identifying patterns and correlations within the dataset, ML algorithms can model the complex relationships between synthesis parameters and the resulting properties of CNTs. These models can predict how changes in synthesis parameters will affect the properties of the resulting CNTs, facilitating the identification of optimal synthesis conditions, significantly reducing the need for trial-and-error approaches and accelerating the discovery of targeted CNTs with desired structural properties. This approach can also provide deeper insights into the underlying mechanisms governing CNT growth.

In CNT synthesis, the parameter space is vast and multidimensional, as listed in Figure 2b. These parameters may interact in non-linear ways to influence the structural properties of CNTs. ML algorithms such as support vector machines (SVM), random forests (RF), XGBoost, multilayer perceptron (MLP), Bayesian optimization, and artificial neural network (ANN) are particularly effective in exploring this parameter space. They can identify complex patterns and correlations that might be missed by traditional statistical methods. These models have been previously applied in material synthesis and showed excellent performance [16, 60-65]. In the field of CNT synthesis, successful applications of data-driven approaches have also been demonstrated [15, 16, 29, 66-70].

For instance, Lin et al. demonstrated a route for addressing the synthetic trade-off between CNT forest crystallinity and growth efficiency through the assistance of data-mining approach [16]. Specifically, synthetic trade-offs in the synthesis of SWCNT forests are very challenging as growing certain desired properties can often come at the expense of other desirable characteristics. One example is the one between crystallinity and growth efficiency, resulting in the difficult of achieving both high crystallinity and tall forest simultaneously (Figure 3a). To address this, Lin et al. used data mining approach to train a machine learning regression model (XGBoost) using nine input feature descriptors with a set of 585 experimental synthesis data (Figure 3b). Subsequently, 16000 exploratory “virtual” experiments were performed by the trained model to examine potential routes toward addressing the current crystallinity–height (growth efficiency) trade-off limitation, and possible growth conditions were predicted (Figure 3c). Finally, validation experiments showed very good agreement with the predictions, highlighting the effectiveness and accuracy of the predictive capability of the ML model, which achieved improved results in less than 50 validation tests. Importantly and fundamentally, the trained model revealed the surprising importance of the nature of the carbon feedstock, as a route for indirectly maintaining a high level of crystallinity at a high growth efficiency through the maintenance of the activity of the catalysts to overcome the trade-off. This data-driven approach represents a significant advance in complex multivariable CNT synthesis systems.

Another example is that Ji et al. used ML for high-throughput screening of the efficient growth of high quality SWCNTs [68]. A database of 1280 experiments was built with 4 input parameters of thickness of cobalt (Co) catalyst film, growth temperature, reduction time, and carbon precursor flow rate and one output of Raman I_G/I_D ratio. ML models including linear regression (LR), random forest regression (RFR), support vector regression (SVR), and ANN were trained and RFR was finally chosen due to its highest prediction performance (Figure 3e). The trained model was used to further explore the parameter space for the optimum growth conditions for high-quality SWCNTs with 38016 combinations of growth parameters (Figure 3f-h). Finally, the predicted optimum growth parameters were validated to achieve a high I_G/I_D value of 138 in conventional CVD growth process. This efficient modeling, predicting, and learning ability of the combined high-throughput and ML method shows great potential to speed up the controlled synthesis of SWCNTs with specific structures and properties.

In the data-driven approach, the size of the dataset plays a crucial role in determining the performance and reliability of ML models. The general thinking is that larger datasets are beneficial for training ML models because they can provide more information for the model to learn from, reducing overfitting, leading to more accurate and robust predictions. However, they also require more computational resources. Sufficient unbiased data is crucial for successful ML training and validation [71]. The appropriate dataset size depends on several factors, including the problem type, the level of complexity, the number of features, data quality and error tolerance. This makes it a case-by-case scenario. The most widely used rule-of-thumb is that the dataset size should be at least 10 times the number of weights in the model. However, other guidelines also exist, such as requiring 50 to 1000 times the number of prediction classes or 10 to 100 times the number of features [72]. Krasnikov et al. examined the implementation of ML techniques and discussed features of the optimal dataset size and density for aerosol synthesis of SWCNTs with a complex carbon source [69]. They originally employed a dataset of 369 points comprising 4 inputs and 3 target parameters and assessed the performance of six ML methods. They showed that even a dataset of 250 points with the inhomogeneous distribution of input parameters is sufficient to reach an acceptable performance of the ANN model, wherein the error is most likely to arise from experimental inaccuracy and hidden uncontrolled variables. Therefore, careful consideration of dataset quality and input feature selection, rather than just dataset size, seems to be more important.

In summary, the use of ML in data-driven optimization of CNT synthesis parameters not only reduces the time and resources required for CNT synthesis experimentations, but also enhances the reproducibility of results. By providing a deeper understanding of the synthesis process, ML enables researchers to design experiments more strategically, leading to the discovery of new synthesis pathways and the production of CNTs with tailored properties.

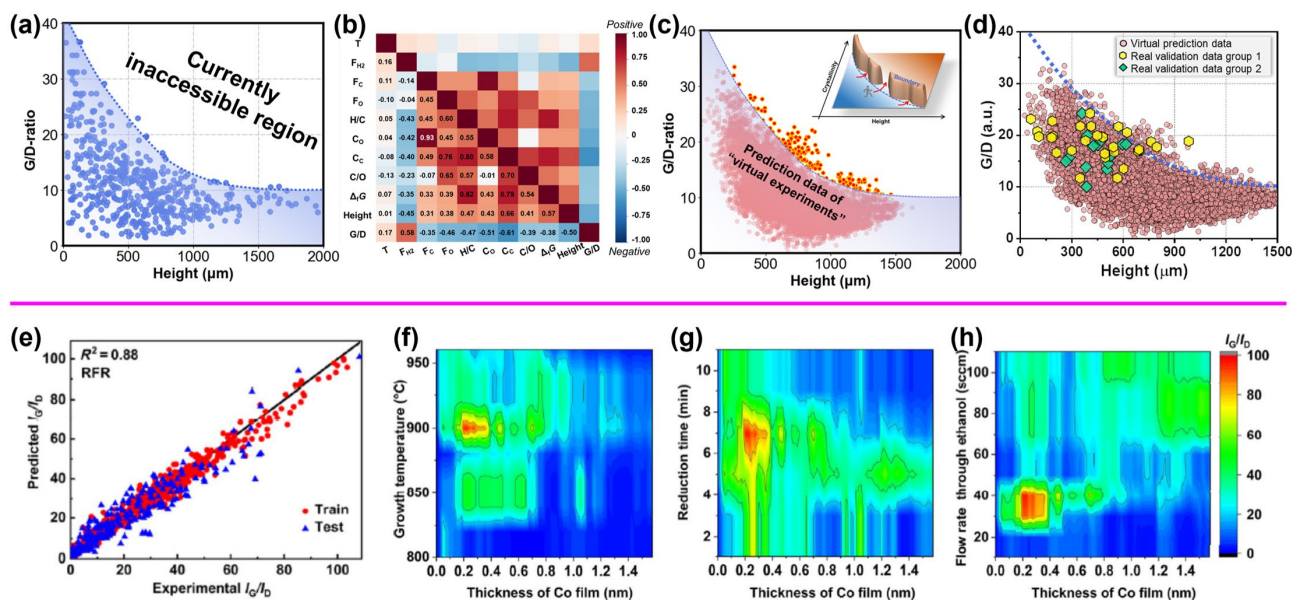


Figure 3. Data-driven optimization for CNT synthesis. (a–d) Data-mining assisted SWCNT forest synthesis overcoming the synthetic trade-off. Reprinted with permission from Reference [16]. (a) Trade-off between G/D ratio and CNT height. (b) Heat map of Pearson correlation coefficient matrix for the nine inputs and two outputs. (c) Plot of virtual experiment data with prediction points beyond the boundary highlighting the successful access to the inaccessible region. (d) Validation experiment results. (e–h) ML assisted SWCNT high-throughput screening for high-quality SWCNTs. Reprinted with permission from Reference [68]. (e) I_G/I_D values from experimental measurements and predictions from the RFR model. Dependence of predicted Raman I_G/I_D on the thickness of Co catalyst film as a primary variable and (f) growth temperature, (g) reduction time, and (h) flow rate through ethanol as secondary variables.

2.2. Autonomous CNT Synthesis

Autonomous synthesis represents a paradigm shift in materials science, where ML and automation technologies are integrated to enable fully automated production/synthesis processes. In the context of CNT synthesis, this involves the development of systems that can autonomously adjust synthesis parameters in real-time based on continuous feedback from ML algorithms, ensuring the production of CNTs with desired, precise and consistent properties. This concept goes beyond traditional methods that rely on manual adjustments and trial-and-error experimentation. Instead, autonomous systems can dynamically adjust synthesis parameters on-the-fly to optimize the quality and yield of CNTs, significantly improving efficiency and reproducibility.

Due to the multivariable nature of CNT synthesis, a closed-loop autonomous synthesis system is uniquely suitable for optimizing the synthesis process continuously and autonomously by integrating real-time data monitoring, ML algorithms, and automated process controls. As conceptually diagrammed in Figure 4a, a simple such system generally starts with a CVD reactor to perform the synthesis process and collect the growth parameters. The system also needs to be equipped with in-situ monitoring and evaluation units, such as Raman spectroscopy, thermogravimetric analysis (TGA), and mass spectrometry, to provide real-time monitoring of the process. Then all these data are sent into a ML control unit to analyze the data and predict the optimal synthesis conditions. Finally, the decisions of new synthesis conditions are set and fed back into the CVD process.

Autonomous CNT synthesis has been successfully demonstrated in several experimental setups [73-76]. For instance, a proof of concept was exemplified by Maruyama et al. with adaptive rapid experimentation and *in situ* spectroscopy (ARES) system (Figure 4b). This system was developed to increase the experimentation rate by 100-fold, to 100 runs per day, with results analyzed in situ and in real time via Raman spectroscopy. Such system was used to synthesize CNTs on the surface of micropillars and linear regression modeling was used to map regions of selectivity toward SWCNT and multiwall CNT (MWCNT) growth in the complex parameter space of 534 CVD experiments [73]. Recently, the same group demonstrated a closed-loop system using Bayesian optimization (BO) as an efficient and robust ML algorithm integrated with the ARES setup (Figure 4b). The CNT growth rates were extracted from the ARES and fed into the BO algorithm. The algorithm then generated a new set of conditions, run by ARES, and the new output data was sent to the BO planner to update the existing dataset and plan a new experiment. Such closed-loop system can significantly improve the predictive power, show good consistency performance, exploit a complex parameter space, and achieve a 5-fold faster experimentation speed than before [75].

More recently, Zhang's group introduced an AI-driven platform, Carbon Copilot (CARCO), which integrates transformer-based language models tailored for carbon materials, robotic CVD, and data-driven ML models. Using CARCO, a catalyst discovery was demonstrated by predicting a superior Titanium-Platinum bimetallic catalyst for high-density horizontally aligned CNT (HACNT) array synthesis, validated through over 500 experiments. With the assistance of millions of virtual experiments, an unprecedented 56.25% precision in synthesizing HACNT arrays with predetermined densities was achieved, within just 43 days [76]. This work exemplifies a great advance towards the integration of AI/ML with human expertise to overcome the limitations of traditional experimental approaches.

In summary, despite of some facing challenges, the implementation of autonomous synthesis systems could revolutionize the CNT research by drastically reducing the time and cost associated with traditional synthesis methods. This approach not only enhances the scalability of CNT production but also allows for the precise control of CNT properties, which is crucial for their integration into commercial applications such as electronics, composites, and biomedical devices.

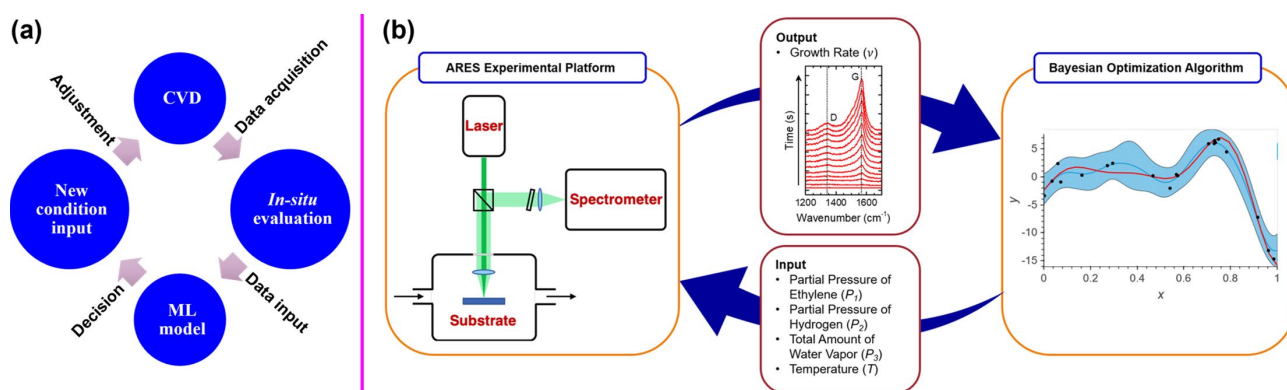


Figure 4. Autonomous CNT synthesis. (a) A conceptual diagram of a closed-loop autonomous CNT synthesis system. (b) A closed-loop autonomous system with adaptive rapid experimentation and *in situ* spectroscopy (ARES) and Bayesian optimization ML algorithm. Reprinted with permission from Reference [75].

3. Machine Learning-Assisted CNT Characterization

The most essential question in materials science including CNT research is to establish the relation of the microstructures with synthesis conditions, physical and chemical properties. Materials characterization is to extract information about the structure, including imaging in real space and spectroscopy in energy space, respectively. By establish the relationship between structure and properties, characterization is essential to understand growth mechanism, design microstructures for desired properties.

For CNTs, structural information extracted from characterization includes purity, morphology, diameter, length, conductivity type, and distribution of chiralities, and so on. Transmission electron microscopy (TEM) was the key for the discovery of CNTs [77], and for the precise characterization of individual CNTs, including the chiral indices [78]. On the other hand, Raman spectroscopy has been widely used for quick and statistical analysis of CNT samples, including purity, distribution of diameter and chirality [79, 80].

In conventional materials characterizations, images and spectra are acquired and analyzed manually one-by-one. It is challenging to reach the optimum acquisition parameters because of the trade-offs in temporal resolution, spatial resolution, field of view, data volume, acquisition speed, stability, irradiation damage, and signal-to-noise ratio (SNR). For CNTs, from images in real space, diameters and lengths are measured. From diffraction patterns in reciprocal space, crystalline structures could be analyzed by measuring the distances and angles of diffraction spots. And from spectra, peak positions are compared with existing spectra in databases to determine the substances. The conventional analysis process is time consuming and biased by human factors.

In recent years, ML has been applied to materials characterizations to automate the analysis process and to recognize the hidden patterns in data [81-86]. It has been demonstrated that ML can enhance the efficiency, increase the accuracy and most importantly to handle large datasets through high-throughput analysis. In this section, ML -assisted CNT characterization will be introduced with examples of rapid identification of Raman spectroscopy and automated chirality determination from TEM Images.

3.1. Machine Learning for Rapid Identification of Raman Spectroscopy

Raman spectroscopy is based on the inelastic scattering of photons with phonons. It is widely used to analyze vibrational modes and to identify molecular structures with the fingerprints in the position, width, shape of the peaks. Raman spectroscopy has been one of the most important methods to characterize CNTs [80]. The purity and quality of CNTs could be extracted from the ratio of G and D bands. In addition, diameter and chirality distribution could be obtained from the radial breathing modes (RBM) modes [79, 87]. One of the challenges for Raman spectroscopy is the low SNR, since inelastic Raman

scattering cross-section is much smaller than the cross-section for elastic Rayleigh scattering. In recent years, ML algorithms have been applied for Raman spectroscopy-based classification and recognition [19, 68, 88, 89].

For instance, Zhang et al. used deep learning to automate and speed up the analysis of Raman spectra to identify the structure features of suspended CNTs, including position, number and metallicity (Figure 5a-f) [88]. The deep learning model was based on a convolutional neural network (CNN) with four convolutional layers, a softmax layer, and a cross-entropy layer for defining the loss function. A database was consisted of 62130 Raman spectra from suspended CNTs. And the samples were labeled as semiconducting (S-CNTs), metallic (M-CNTs), and empty trenches (no CNTs). The CNN was trained on the dataset and tested on a separate validation set of 48887 spectra. After training the CNN, softmax thresholding was applied to refine the classification, to reduce the number of false positives, and to enhance the accuracy. The model achieved a classification accuracy of 90% for spectra with the SNR values as low as 0.9, and the accuracy was up to 98% for higher SNRs. The accuracy was found to increase with longer integration times (>30 ms) and higher laser power, with a maximum of 99% at 1 mW laser power. The deep learning-assisted rapid identification of CNT structures from Raman spectroscopy can be integrated into industrial production lines for real-time monitoring of CNTs growth.

In another example, Kajendarajah et al demonstrated a rapid diagnosis and analysis of tip-enhanced Raman spectroscopy (TERS) mappings of individual CNTs using deep learning neural networks [89]. In this work, TERS maps were measured on SWCNTs. TERS spatial resolution together with spectral selectivity is used to facilitate discrimination of semiconductive *versus* metallic characteristics of SWCNTs, the identification of bundles, and the identification of defect areas. Two multi-purpose ANNs were created and utilized to characterize SWCNTs. Using Raman spectra gathered from TERS experiments, ANN Model 1 classified each spectrum as background or CNT with an associated confidence percentage. ANN Model 2 provided clear and rapid filtering of the three vibrational modes of CNTs. For any given CNT Raman spectrum, ANN Model 2 accurately identified the existence of these modes. Both ANN Model 1 and Model 2 were used to generate TERS maps with enhanced contrast. ANN Model 1 and ANN Model 2 worked synergistically to identify the number and the assignments associated with the different SWCNTs vibrational modes. In addition, the developed approach enables enhanced visualization of CNT defect areas. The methodologies used to create the deep learning ANNs have resulted in a 98% accuracy for ANN Model 1 and 96% accuracy for ANN Model 2. The approach performed a diagnosis of unseen raw TERS hyperspectral data in only 4 to 6 hours for a spectral cube composed of 8000–10 000 set of spectra with 1600 points each.

In summary, the utilization of ML has enabled a fast and accurate identification and classification of CNTs combing with Raman spectroscopy, resulting in a powerful and comprehensive analysis tool.

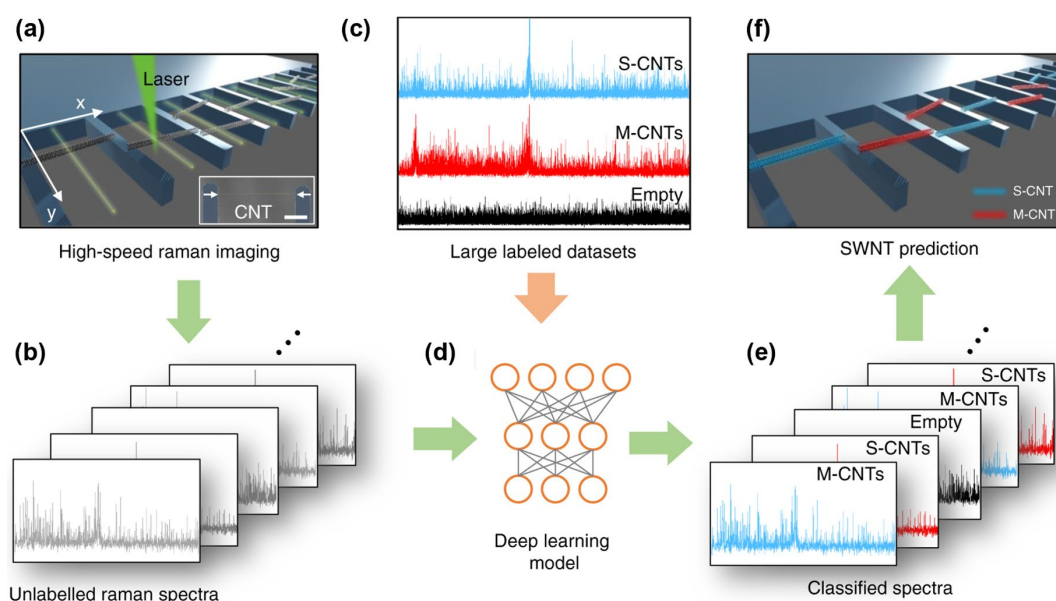


Figure 5. Deep learning-assisted rapid identification of Raman spectra from suspended CNTs. (a) Raman imaging. (b) Data collection. (c) Raman spectra database labeling. (d) CNN deep learning model. (e) Training and classification. (f) CNT identification. Reprinted with permission from Reference [88].

3.2. Machine Learning for Automated Chirality Determination from TEM Images

TEM is a key instrument for characterizing nanomaterials such as CNTs. It combines multiple functions, ranging from imaging with atomic resolution, chemical analysis of individual atom, mapping of local physical properties, to fabrication with nanometer or even atomic precision.

For CNTs, it is quite a challenge to operate a modern TEM to precisely characterize the atomic structures, because of the small atomic mass, small diameter, and complex circular geometry. It takes years to train a professional microscopist to master the variety of skills, including high-resolution TEM (HRTEM) imaging, nano-beam electron diffraction for chiral indices, STEM imaging and 4D-STEM for probing local structures and properties.

In recent years, ML methods have been applied to electron microscopy, ranging from data modelling and data analysis to atomic fabrication [27, 90–94]. For example, Lin et al. quantified the fluctuations in catalyst carbon content by using an automated, atomic-scale structural analysis of the time-resolved ETEM images. Such fluctuations in the composition of catalysts were correlated with the SWCNT growth rate [28]. Förster et al. developed a deep learning approach for determining the chiral indices of CNTs from HRTEM images (Figure 6a) [93]. Since the chiral indices entirely determine the atomic structures, electronic and optical properties, it is critical to identify the chiral indices of individual CNTs and more important for the statistical distribution of chirality in a CNT sample. Electron diffraction is the most precise method to determine CNTs' chiral indices, however, individual CNTs as long as 100 nm are required. In this work, Förster decided to use HRTEM images to determine the CNTs chiralities, since sub-angstrom resolution is achievable for modern Cs-corrected TEMs.

Due to the lack of enough high-quality experimental images of CNTs, a database was constructed by high-throughput atomistic structural simulation and followed by TEM simulations to generate HRTEM images. To increase the diversity of the data and generality of the model, variability was included, such as position, orientation, magnification, defocus, aberration, noise, and so on. In total, all possible 261 chiral indices for the CNTs with diameter of 0.48 nm to 2.30 nm were considered. And for each chirality, 5000 images were simulated to general a database of 1.3 million images. A CNN based on LeNet-5 was

392

393

394

395

396

397

398

399

400

401

402

403

404

405

406

407

408

409

410

411

412

413

414

415

416

417

418

419

420

421

422

423

424

425

426

427

used to model and classify simulated TEM images to identify the chiral indices. To enhance the modelling precision, two CNNs were used for the diameter and chirality, respectively. The first CNN could determine the diameter with an accuracy of 99 %. And an overall accuracy of 90.5% was found for the second CNN in classifying chiral indices. The CNN based chirality classification system was evaluated by using experimental HRTEM images. When images of sufficiently high quality were used, 71% of the results were consistent for classification done manually and automatically.

In this pioneering work, ML has demonstrated enhanced efficiency to identify the chiral indices, which typically takes 15-30 minutes to analyze one picture manually. And the model showed a high robustness, for the nanotubes with defects. This method opens the door for high-throughput analysis of HRTEM images to get insight into the distribution of chirality to understand the growth mechanism of CNTs.

As is well known, the structures of CNTs are predominantly determined by the characteristics of the catalyst. Therefore, analyzing catalyst nanoparticles is essential to understanding the CNT growth mechanisms. However, due to their dynamic nature and nanoscale size, quantitatively studying nanoparticle morphologies and conducting statistical analyses on them is extremely challenging. Recently, Lee et al. developed a mass-throughput method for analyzing nanoparticle morphologies by applying a genetic algorithm to an image analysis technique (Figure 6b) [94]. This approach enabled the analysis of over 150000 nanoparticles with a high precision of 99.75% and a low false discovery rate of 0.25%. The study also introduced clustering techniques to group nanoparticles with similar morphological shapes for extensive statistical analysis. It was determined that analyzing at least 1500 nanoparticles is required to represent the total nanoparticle population at a 95% credible interval. Additionally, the number of TEM images and the average number of nanoparticles per image should be considered to ensure a representative sample. The statistical distribution of polydisperse nanoparticles was also found to be critical in accurately estimating their optical properties.

In summary, combing ML with TEM techniques not only enhances the efficiency and accuracy of CNT analysis but also enables precise characterization of catalyst nanoparticle morphology. This integration provides a powerful tool to significantly advance the field of CNT research.

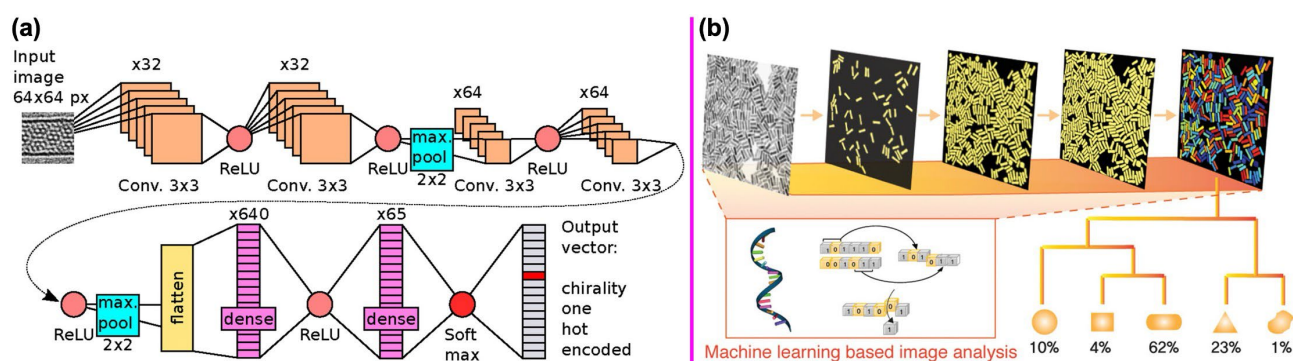


Figure 6. (a) Architecture of the CNNs for determining the chiral indices of CNTs from HRTEM images. Reprinted with permission from Reference [93]. (b) Statistical characterization of the morphologies of nanoparticles through ML-assisted TEM image analysis. Reprinted with permission from Reference [94].

4. Machine Learning-Assisted CNT Applications

Besides the application in CNT synthesis, ML also plays a crucial role in enhancing the CNT applications across various fields to improve their integration into devices and materials and predict their performance. This section explores how ML aids CNT applications in electronics and sensors, composite materials, and the biomedical field.

4.1. CNT Applications in Electronics and Sensors

CNTs possess exceptional electrical properties, such as high conductivity, ballistic transport, and excellent current-carrying capacity, making them ideal for electronic devices and sensors [31]. However, integrating CNTs into practical devices requires precise control over their properties, processing, and placement, which can be challenging due to their nanoscale dimensions and variability in structural properties. ML can help overcome the challenges by providing data-driven insights and optimization strategies [95-101].

For instance, Tadokoro et al. demonstrated a simple and AI-assisted method for the more efficient fabrication of a massive CNT-based nanocantilever (Figure 7a), compared to traditional fabrication methods using CVD and/or dielectrophoresis, which generally contain manual, time-consuming processes such as the placing of additional electrodes and careful observation of single-grown CNTs [97]. They trained deep neural network to recognize the randomly positioned single CNTs on the substrate, measure their positions, and determine the edge of the CNT on which an electrode should be clamped to form a nanocantilever. This AI assistance significantly improved the recognition and measurement processes, 2 sec versus 12 h by manual processing.

Another example is that Aliyana et al. utilized ML approach to accurately correlate the impedance variations in zinc oxide/MWCNT nanocomposite (F-MWCNT/ZnO-NFs) to NH_4^+ ion concentrations [98]. The proposed NH_4^+ sensor along with the decision-making ML model can identify and operate at specific operating frequencies to continuously collect the most relevant information from a system (Figure 7b). In addition, Bian et al. utilized ML techniques (LR, RF) to create a calibration method for Hg^{2+} sensors based on CNT field-effect transistor (FET) devices (Figure 7c) to solve sensor response saturation [99]. Such application of ML techniques to investigate which features in the FET signal maximally correlate with concentration changes provide valuable insight into the CNT sensing mechanism and assist in the rational design of future nanosensors. Furthermore, Fan et al. proposed an efficient framework for optimizing the design of CNT FET through the integration of device physics, ML, and multi-objective optimization to expedite the early-stage development of advanced transistors [100]. Moreover, Kelich et al. trained ML models (convolutional neural network, SVN) to predict DNA sequences with strong optical response to neurotransmitter serotonin (Figure 7d). They discovered five DNA-SWCNT sensors with higher fluorescence intensity response than those using only manual screening method [101].

In summary, these studies collectively highlight the transformative potential of ML approaches in advancing the development of CNT applications in electronics and sensors. These examples underscore the potential of ML to not only solve specific technical challenges but also to revolutionize the entire process of CNT-based device development. By automating complex analyses, optimizing sensor design, and providing rapid, data-driven insights, ML approaches are poised to play a pivotal role in accelerating the innovation and deployment of CNT technologies in various electronic and sensing applications.

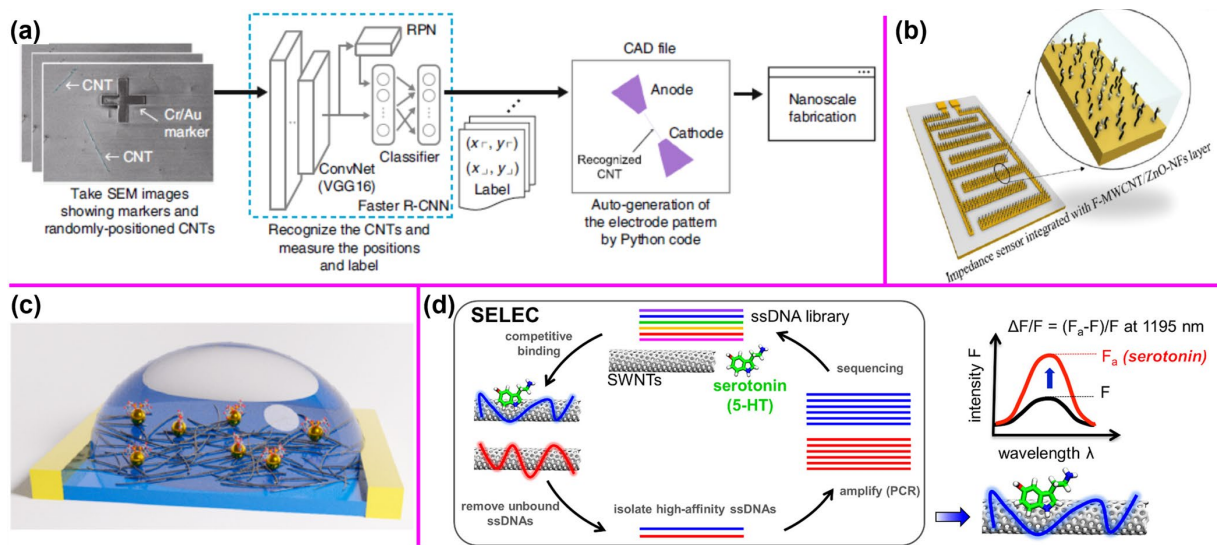


Figure 7. (a) AI-assisted framework for fabricating nanocantilevers, using a neural network to recognize CNTs and a Python code to generate electrode patterns, and the final massive fabrication process. Reprinted with permission from Reference [97]. (b) NH₄⁺ selective impedance sensors fabricated by embedding F-MWCNT/ZnO-NF active layers on interdigitated arrays. Reprinted with permission from Reference [98]. (c) Schematic diagram for the composition of sensing material and liquid-gated CNT FET. Reprinted with permission from Reference [99]. (d) ML-assisted approach to identify DNA sequences in DNA-SWCNT conjugates with high serotonin response. Reprinted with permission from Reference [101].

4.2. CNT Applications in Composite Materials

CNTs are widely used in composite materials to enhance their mechanical, thermal, and electrical properties [45]. However, achieving uniform dispersion and proper alignment of CNTs within the composite matrix is challenging due to the strong van der Waals forces between the nanotubes and their tendency to agglomerate. ML provides powerful tools to optimize these processes and predict the resulting composite properties, thereby enhancing the performance of CNT-based composites across various applications [102-112].

For instance, Yu et al. utilized ML techniques to explore the structure-property linkages of CNT-reinforced AlSi10Mg nanocomposites [102]. The proposed processing framework pipeline starts with SEM image processing of cellular microstructural features, followed by training of ML models (AdaBoost, gradient tree boosting, K-nearest neighbors, decision tree, and extra trees regressors), and property prediction (Figure 8a). The developed models demonstrated satisfactory performance, with the extra trees regression model predicting hardness with a 2.47% error and the decision tree regression model predicting relative mass density with a 1.42% error. This framework can be applied to process optimization and mechanical property manipulation for designing new alloys or composites.

In another example, Ranaiefar et al. investigated structures and mechanical property predictions of CNT-reinforced acrylonitrile butadiene styrene (ABS) composites fabricated by 3D-printing using ML approach [103]. Multiple regression algorithms were evaluated, including ridge regressor, linear regression, k-neighbors regressor, gradient boosting regressor, random forest regressor, extra trees regressor, decision tree regressor, and lasso regression. The predictive classification and regression supervised ML models supported the experimental results with 0.92 accuracy and a 0.96 coefficient of determination (Figure 8b). This approach utilizing ML techniques can help inform and guide the design of 3D-printed structures for targeted performance.

Furthermore, Jalal et al. demonstrated a concept of 'Big Data' analytics in composite structure with focusing on functionally graded CNT-reinforced composites (FG-CNTRC)

using a mesh-free method and an optimized neural network (ONN) approach to study the effect of structural parameters on vibrational frequency [104]. They built a big data containing 15625 entries with six parameters and developed an optimized ONN model for predictive modeling. The ONN model demonstrated computation speeds thousands of times faster than the mesh-free method while keeping a simulation error as low as 1%, suggesting it is an efficient and reliable approach for handling big data in the optimization and design of composites.

Moreover, different ML techniques have been utilized to study various CNT-based composites for property improvements either in combination with experimental investigations, such as CNT-reinforced cementitious composites [105-107], CNT-reinforced polymeric composites [108-111], or alongside computer simulations [112].

In summary, ML is revolutionizing the development and application of CNT-based composite materials by providing powerful tools for optimizing fabrication processes, predicting composite properties, and guiding the design of composites with tailored performance characteristics. By leveraging large datasets and advanced ML algorithms, researchers can overcome the challenges associated with CNT dispersion and alignment, enabling the production of high-performance composites for a wide range of applications. As ML technologies continue to evolve, their integration with composite material research and manufacturing processes will likely lead to even greater advancements in this field.

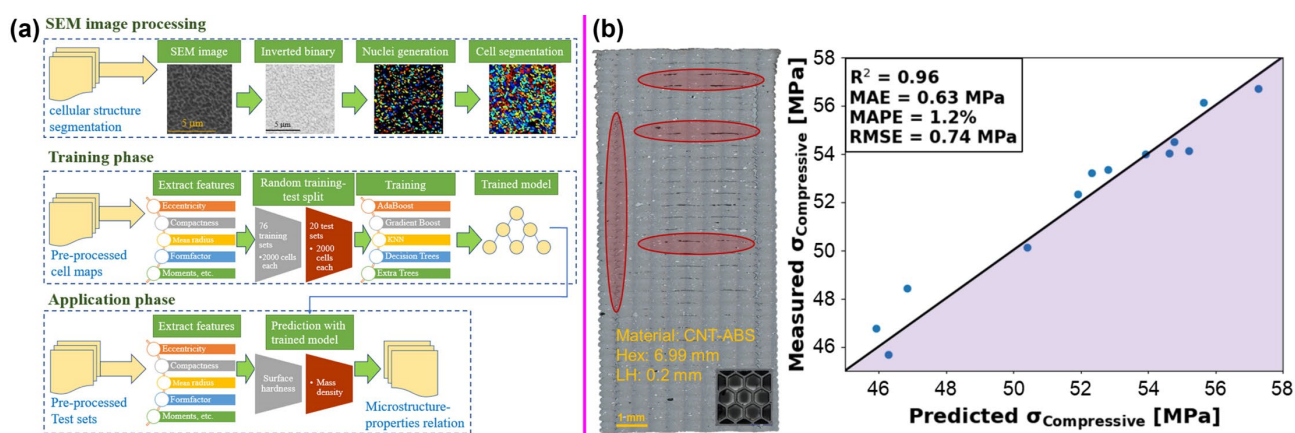


Figure 8. (a) Schematic of the proposed processing framework pipeline for AlSi10Mg nanocomposites microstructure-properties linkages. Reprinted with permission from Reference [102]. (b) Optical microscopy cross-sections, in-plane with the print direction, of CNT reinforced ABS honeycomb composite and predicted ultimate compressive strength from trained linear regression model evaluated against experimental measurements. Reprinted with permission from Reference [103].

4.3. CNT Applications in the Biomedical Field

CNTs also possess unique properties, such as high surface area, biocompatibility, and the ability to penetrate cell membranes, making them ideal for various biomedical applications [42, 113]. ML enhances these applications by providing tools for optimizing the design of CNT functionalization, predicting their interactions with biological molecules, enabling high-throughput selection of targeted DNA sequences, accelerating the discovery of effective biomolecular constructs, and even predicting their genotoxicity [114-118].

For instance, Ouassil et al. developed a random forest classifier (RFC, Figure 9a) to investigate the relationship between a protein's amino acid sequence and a protein's binding propensity to SWCNTs [114]. The classifier aimed to predict which protein-SWCNT interactions to expect in biological environments and to predict high-affinity protein binders to SWCNTs, along with protein features associated with such binding affinity to improve the process of protein-nanoparticle construct design (Figure 9b). The model was validated with a new set of proteins by performing quantitative protein adsorption

experiments. The ML classifier can serve as a useful tool for understanding how protein sequences influence nanotube binding.

Additionally, the use of single-stranded DNA (ssDNA) as a wrapping surfactant for SWCNTs is a promising approach to functionalize and modify the SWCNT surface, enabling precise control over SWCNT alignment. This approach has shown great potential in biomedical applications, including drug delivery, gene therapy, and biosensors. Lee et al. employed high-throughput systematic selection of high-affinity ssDNA sequences using ML models (RF, MLP, CNN, etc.) from a vast random library (Figure 9c). The model accurately distinguished high-affinity ssDNA sequences and provided predictive capabilities for binding affinity, supporting the design of tailored DNA-SWCNT constructs. The stability of ssDNA conformations on SWCNTs were validated by molecular dynamics simulations[115].

Furthermore, the prerequisite of utilizing DNA in sequence-dependent applications, such as biomedical sensor, is to search specific sequences, which represents a significant challenge due to the countless possible sequence combinations. Lin et al. demonstrated an ML assisted experimental method for systematically searching DNA sequences based on sequence-dependent recognition between DNA and SWCNTs (Figure 9d). Compared with empirical search methods, their approach significantly improved both the number of resolvable sequences and the success rate of finding them, from $\sim 10^2$ to $\sim 10^3$ and from $\sim 10\%$ to $>90\%$, respectively [116]. Moreover, ML approaches have also been successfully used to investigate CNT genotoxicity prediction [117] and discover molecular recognition based on SWCNT corona phases [118].

In summary, ML techniques enhance CNT applications in the biomedical field by enabling precise and targeted functionalization of CNTs, improving their biocompatibility, and optimizing their interaction with biological systems. Additionally, ML-driven approaches provide powerful predictive tools to accelerate the discovery and development of CNT-based biomedical constructs, expanding the possibilities for innovative therapies and diagnostics.

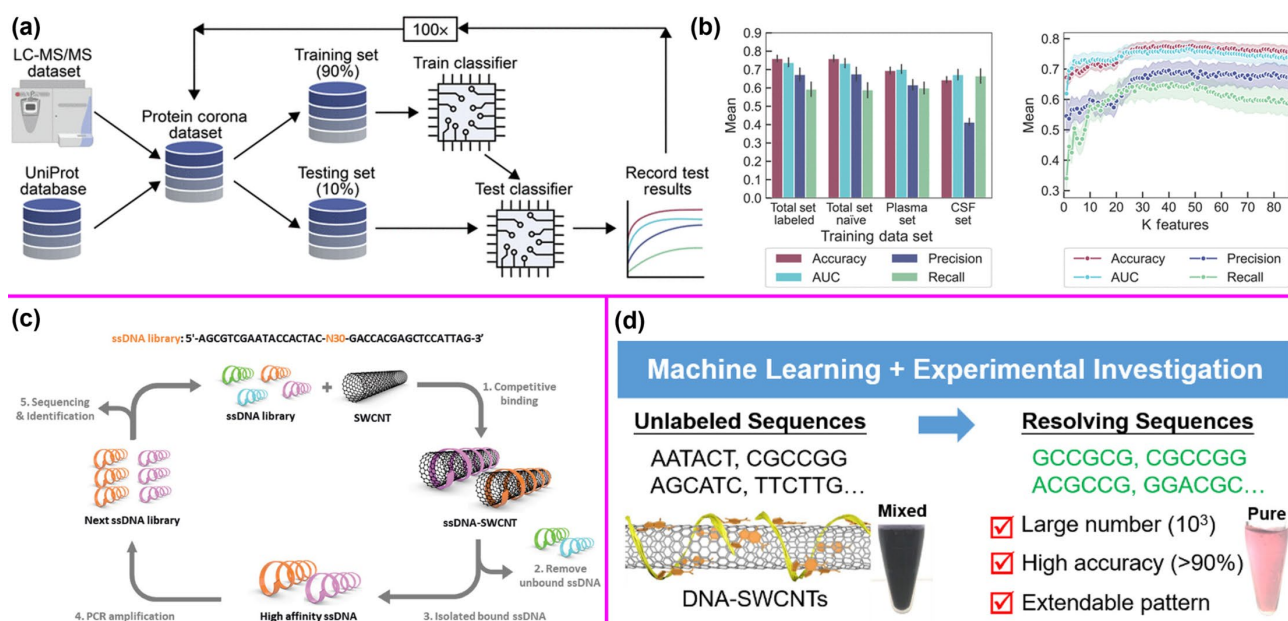


Figure 9. (a) RFC workflow and (b) classifier performance results on different biofluid training datasets and with varied protein feature inputs. Reprinted with permission from Reference [114]. (c) Selection of high-affinity ssDNA sequences on SWCNT surfaces. Reprinted with permission from Reference [115]. (d) ML assisted systematic search of DNA sequences. Reprinted with permission from Reference [116].

590

591

592

593

594

595

596

597

598

599

600

601

602

603

604

605

606

607

608

609

610

611

612

613

614

615

616

617

618

619

620

621

622

623

624

625

5. Conclusion and Perspective

This review demonstrates the transformative impact of ML on CNT research, spanning optimization of growth conditions, automation of structure characterization, to application development. ML algorithms have proven highly effective in modeling the complex relationships between synthesis parameters and the resulting structures and properties of CNTs, by identifying patterns and correlations within the dataset. As a result, the height of CNT forests and the quality of CNT thin films were effectively improved. In addition, the integration of autonomous systems has further enhanced the growth production, reducing reliance on manual trial-and-error processes.

ML has been widely adopted for materials characterization and has started to revolutionize the CNT field by automating traditionally manual tasks. Successful applications include determination of the chiral indices through HRTEM images and rapid identification of suspended CNTs using Raman spectroscopy, both of which used deep learning for automation. ML has demonstrated the enhanced efficiency to extract information to automate the analysis process, markedly improving the speed and accuracy of data analysis, facilitating high-throughput studies and more consistent results.

Moreover, ML has been accelerating the innovation and deployment of CNT-based applications in electronics and sensors, through automating complex analyses, optimizing sensor design, and providing rapid, data-driven insights. ML has provided valuable guidance to design composites with desired properties, through optimizing fabrication processes, predicting composite properties. In the biomedical field, ML is playing a crucial role in optimizing CNT functionalization and predicting their interactions with biological molecules, furthering CNT applications in drug delivery, biosensors, and diagnostics.

Despite the significant progress, the integration of ML in CNT research is still in its early stages and holds immense potential for exponential growth in the near future. Up to now, application examples of ML in CNT characterizations are still very few. A search using the key words “machine learning” and “carbon nanotube” in the “Web of Science Core Collection” reveals only 131 publications, with the number of publications increases in a linear manner from 2 in 2015 to >30 in 2024.

One of the main limitations is the lack of organized data, which is indispensable for training complex ML models. Currently, there is no centralized database for CNT research to include experimental data from various groups, with most advances being driven by individual groups accumulating years of experimental data. The hunger for data is a common challenge in data-driven science. Typically, a scale of tens of thousands of data points is required for high accuracy modelling of deep learning. However, it is time consuming to do experiments. It takes hours to grow, seconds to take TEM images, and milliseconds to obtain a Raman spectrum. Collaboration in CNT research community, among experimentalists, theorists, and data scientists will be the key to construct shared CNT databases and establish protocols for data storage, sharing, using, and importantly protecting the precious data.

As a subset of ML, generative AI has gained a lot of attention, since it not only learns but also generates new content, such as text and images, based on training data. In recent years, natural language processing (NLP) models like GPT-4 can generate human-like text and engage in conversations. Generative AI has been started to be applied to scientific research including materials science, though the applications in CNT research are still few. The potential for such tools is immense and should not be overlooked. Generative AI models, such as generative adversarial networks (GANs) and variational autoencoders (VAEs), could be highly useful in future CNT research for tasks like optimizing synthesis pathways, predicting novel CNT structures, and enabling property-driven material discovery. The integration of generative AI into CNT research has the potential to further accelerate innovation by automating more creative aspects of material design and discovery. As this area develops, we anticipate that generative AI will play a pivotal role alongside ML, opening new frontiers in CNT research.

Looking ahead, another important direction will be the development of integrated AI systems that combine growth optimization, structural characterization, and property measurements into a single closed-loop framework. By leveraging ML techniques, these systems could continuously optimize the entire CNT research process, significantly accelerating discovery and innovation. As human researchers shift their focus to designing AI systems and making key scientific judgments, this integrated AI-driven approach is expected to lead to revolutionary breakthroughs in CNT growth mechanisms, novel structures, and unprecedented applications.

Author Contributions: “Conceptualization, G.C. and D.T.; investigation, G.C. and D.T.; writing—original draft preparation, G.C. and D.T.; writing—review and editing, G.C. and D.T.; visualization, G.C.; funding acquisition, G.C. and D.T. All authors have read and agreed to the published version of the manuscript.

Funding: This work was supported by JSPS KAKENHI Grant Number JP23K04552. D.T. discloses support from JSPS Kakenhi (grants JP25820336, JP20K05281, JP23H01796), JST-FOREST Program (grant JPMJFR223T, Japan), WPI-MANA ‘Challenging Research Program (CRP)’, NIMS ‘Support system for curiosity-driven research’, and “Advanced Research Infrastructure for Materials and Nanotechnology in Japan (ARIM)” of the Ministry of Education, Culture, Sports, Science and Technology (MEXT). Proposal Number JPMXP1224NM5238.

Data Availability Statement: Not applicable.

Conflicts of Interest: The authors declare no conflicts of interest.

References

1. Mjolsness, E.; DeCoste, D. Machine learning for science: State of the art and future prospects. *Science* **2001**, *293*, 2051-2055, <https://doi.org/10.1126/science.293.5537.2051>.
2. Ramprasad, R.; Batra, R.; Pilania, G.; Mannodi-Kanakkithodi, A.; Kim, C. Machine learning in materials informatics: recent applications and prospects. *npj Comput Mater* **2017**, *3*, 54, <https://doi.org/10.1038/s41524-017-0056-5>.
3. Jose, R.; Ramakrishna, S. Materials 4.0: Materials big data enabled materials discovery. *Appl Mater Today* **2018**, *10*, 127-132, <https://doi.org/10.1016/j.apmt.2017.12.015>.
4. Jordan, M.I.; Mitchell, T.M. Machine learning: Trends, perspectives, and prospects. *Science* **2015**, *349*, 255-260, <https://doi.org/10.1126/science.aaa8415>.
5. Butler, K.T.; Davies, D.W.; Cartwright, H.; Isayev, O.; Walsh, A. Machine learning for molecular and materials science. *Nature* **2018**, *559*, 547-555, <https://doi.org/10.1038/s41586-018-0337-2>.
6. Huang, G.N.; Guo, Y.N.; Chen, Y.; Nie, Z.W. Application of Machine Learning in Material Synthesis and Property Prediction. *Materials* **2023**, *16*, 5977, <https://doi.org/10.3390/ma16175977>.
7. Xu, P.C.; Ji, X.B.; Li, M.J.; Lu, W.C. Small data machine learning in materials science. *npj Comput Mater* **2023**, *9*, 42, <https://doi.org/10.1038/s41524-023-01000-z>.
8. Wei, J.; Chu, X.; Sun, X.-Y.; Xu, K.; Deng, H.-X.; Chen, J.; Wei, Z.; Lei, M. Machine learning in materials science. *InfoMat* **2019**, *1*, 338-358, <https://doi.org/10.1002/inf2.12028>.
9. Choi, R.Y.; Coyner, A.S.; Kalpathy-Cramer, J.; Chiang, M.F.; Campbell, J.P. Introduction to Machine Learning, Neural Networks, and Deep Learning. *Transl Vis Sci Techn* **2020**, *9*, 14, <https://doi.org/10.1167/tvst.9.2.14>.
10. Sarker, I.H. Machine Learning: Algorithms, Real-World Applications and Research Directions. *SN Computer Science* **2021**, *2*, 160, <https://doi.org/10.1007/s42979-021-00592-x>.
11. Rickman, J.M.; Lookman, T.; Kalinin, S.V. Materials informatics: From the atomic-level to the continuum. *Acta Mater.* **2019**, *168*, 473-510, <https://doi.org/10.1016/j.actamat.2019.01.051>.
12. Raccuglia, P.; Elbert, K.C.; Adler, P.D.F.; Falk, C.; Wenny, M.B.; Mollo, A.; Zeller, M.; Friedler, S.A.; Schrier, J.; Norquist, A.J. Machine-learning-assisted materials discovery using failed experiments. *Nature* **2016**, *533*, 73-76, <https://doi.org/10.1038/nature17439>.
13. Tshitoyan, V.; Dagdelen, J.; Weston, L.; Dunn, A.; Rong, Z.Q.; Kononova, O.; Persson, K.A.; Ceder, G.; Jain, A. Unsupervised word embeddings capture latent knowledge from materials science literature. *Nature* **2019**, *571*, 95-98, <https://doi.org/10.1038/s41586-019-1335-8>.
14. Rao, Z.Y.; Tung, P.Y.; Xie, R.W.; Wei, Y.; Zhang, H.B.; Ferrari, A.; Klaver, T.P.C.; Körmann, F.; Sukumar, P.T.; da Silva, A.K.; Chen, Y.; Li, Z.M.; Ponge, D.; Neugebauer, J.; Gutfleisch, O.; Bauer, S.; Raabe, D. Machine learning-enabled high-entropy alloy discovery. *Science* **2022**, *378*, 78-84, <https://doi.org/10.1126/science.abo4940>.

15. Rao, R.; Carpena-Nunez, J.; Nikolaev, P.; Susner, M.A.; Reyes, K.G.; Maruyama, B. Advanced machine learning decision policies for diameter control of carbon nanotubes. *npj Comput Mater* **2021**, *7*, 157, <https://doi.org/10.1038/s41524-021-00629-y>. 732-733
16. Lin, D.; Muroga, S.; Kimura, H.; Jintoku, H.; Tsuji, T.; Hata, K.; Chen, G.H.; Futaba, D.N. Addressing the Trade-Off between Crystallinity and Yield in Single-Walled Carbon Nanotube Forest Synthesis Using Machine Learning. *ACS Nano* **2023**, *17*, 22821-22829, <https://doi.org/10.1021/acsnano.3c07587>. 734-736
17. Burnett, T.L.; Withers, P.J. Completing the picture through correlative characterization. *Nat. Mater.* **2019**, *18*, 1041-1049, <https://doi.org/10.1038/s41563-019-0402-8>. 737-738
18. Pagan, D.C.; Phan, T.Q.; Weaver, J.S.; Benson, A.R.; Beaudoin, A.J. Unsupervised learning of dislocation motion. *Acta Mater.* **2019**, *181*, 510-518, <https://doi.org/10.1016/j.actamat.2019.10.011>. 739-740
19. Qi, Y.P.; Hu, D.; Jiang, Y.C.; Wu, Z.P.; Zheng, M.; Chen, E.X.; Liang, Y.; Sadi, M.A.; Zhang, K.; Chen, Y.P. Recent Progresses in Machine Learning Assisted Raman Spectroscopy. *Adv Opt Mater* **2023**, *11*, 2203104, <https://doi.org/10.1002/adom.202203104>. 741-742
20. Guo, S.X.; Popp, J.; Bocklitz, T. Chemometric analysis in Raman spectroscopy from experimental design to machine learning-based modeling. *Nat. Protoc.* **2021**, *16*, 5426-5459, <https://doi.org/10.1038/s41596-021-00620-3>. 743-744
21. Menevseoglu, A.; Entrenas, J.A.; Gunes, N.; Dogan, M.A.; Pérez-Marín, D. Machine learning-assisted near-infrared spectroscopy for rapid discrimination of apricot kernels in ground almond. *Food Control* **2024**, *159*, 110272, <https://doi.org/10.1016/j.foodcont.2023.110272>. 745-747
22. Windarsih, A.; Jatmiko, T.H.; Anggraeni, A.S.; Rahmawati, L. Machine learning-assisted FT-IR spectroscopy for identification of pork oil adulteration in tuna fish oil. *Vib. Spectrosc.* **2024**, *134*, 103715, <https://doi.org/10.1016/j.vibspec.2024.103715>. 748-749
23. Penfold, T.; Watson, L.; Middleton, C.; David, T.; Verma, S.; Pope, T.; Kaczmarek, J.; Rankine, C. Machine-learning strategies for the accurate and efficient analysis of x-ray spectroscopy. *Mach Learn-Sci Techn* **2024**, *5*, 021001, <https://doi.org/10.1088/2632-2153/ad5074>. 750-752
24. Drera, G.; Kropf, C.M.; Sangaletti, L. Deep neural network for x-ray photoelectron spectroscopy data analysis. *Mach Learn-Sci Techn* **2020**, *1*, 015008, <https://doi.org/10.1088/2632-2153/ab5da6>. 753-754
25. de Curtò, J.; de Zarzà, I.; Roig, G.; Calafate, C.T. Large Language Model-Informed X-ray Photoelectron Spectroscopy Data Analysis. *Food Control* **2024**, *5*, 181-201, <https://doi.org/10.3390/signals5020010>. 755-756
26. Pielsticker, L.; Nicholls, R.L.; DeBeer, S.; Greiner, M. Convolutional neural network framework for the automated analysis of transition metal X-ray photoelectron spectra. *Anal. Chim. Acta* **2023**, *1271*, 341433, <https://doi.org/10.1016/j.aca.2023.341433>. 757-758
27. Dee, N.T.; Schneider, M.; Zakharov, D.N.; Kidambi, P.R.; Hart, A. Automated processing of environmental transmission electron microscopy images for quantification of thin film dewetting and carbon nanotube nucleation dynamics. *Carbon* **2022**, *192*, 249-258, <https://doi.org/10.1016/j.carbon.2022.02.019>. 759-761
28. Lin, P.A.; Gomez-Ballesteros, J.L.; Burgos, J.C.; Balbuena, P.B.; Natarajan, B.; Sharma, R. Direct evidence of atomic-scale structural fluctuations in catalyst nanoparticles. *J. Catal.* **2017**, *349*, 149-155, <https://doi.org/10.1016/j.jcat.2017.03.009>. 762-763
29. Hajilounezhad, T.; Bao, R.; Palaniappan, K.; Bunyak, F.; Calyam, P.; Maschmann, M.R. Predicting carbon nanotube forest attributes and mechanical properties using simulated images and deep learning. *npj Comput Mater* **2021**, *7*, 134, <https://doi.org/10.1038/s41524-021-00603-8>. 764-766
30. Cao, B.; Adutwum, L.A.; Oliynyk, A.O.; Lubner, E.J.; Olsen, B.C.; Mar, A.; Buriak, J.M. How To Optimize Materials and Devices via Design of Experiments and Machine Learning: Demonstration Using Organic Photovoltaics. *ACS Nano* **2018**, *12*, 7434-7444, <https://doi.org/10.1021/acsnano.8b04726>. 767-769
31. Tang, D.-M.; Erohin, S.V.; Kvashnin, D.G.; Demin, V.A.; Cretu, O.; Jiang, S.; Zhang, L.; Hou, P.-X.; Chen, G.H.; Futaba, D.N.; Zheng, Y.; Xiang, R.; Zhou, X.; Hsia, F.-C.; Kawamoto, N.; Mitome, M.; Nemoto, Y.; Uesugi, F.; Takeguchi, M.; Maruyama, S.; Cheng, H.-M.; Bando, Y.; Liu, C.; Sorokin, P.B.; Golberg, D. Semiconductor nanochannels in metallic carbon nanotubes by thermomechanical chirality alteration. *Science* **2021**, *374*, 1616-1620, <https://doi.org/10.1126/science.abi8884>. 770-773
32. LeMieux, M.C.; Roberts, M.; Barman, S.; Jin, Y.W.; Kim, J.M.; Bao, Z.N. Self-sorted, aligned nanotube networks for thin-film transistors. *Science* **2008**, *321*, 101-104, <https://doi.org/10.1126/science.1156588>. 774-775
33. Feng, C.; Liu, K.; Wu, J.S.; Liu, L.; Cheng, J.S.; Zhang, Y.Y.; Sun, Y.H.; Li, Q.Q.; Fan, S.S.; Jiang, K.L. Flexible, Stretchable, Transparent Conducting Films Made from Superaligned Carbon Nanotubes. *Adv. Funct. Mater.* **2010**, *20*, 885-891, <https://doi.org/10.1002/adfm.200901960>. 776-778
34. Choi, W.B.; Jin, Y.W.; Kim, H.Y.; Lee, S.J.; Yun, M.J.; Kang, J.H.; Choi, Y.S.; Park, N.S.; Lee, N.S.; Kim, J.M. Electrophoresis deposition of carbon nanotubes for triode-type field emission display. *Appl. Phys. Lett.* **2001**, *78*, 1547-1549, <https://doi.org/10.1063/1.1349870>. 779-781
35. Chen, G.H.; Shin, D.H.; Iwasaki, T.; Kawarada, H.; Lee, C.J. Enhanced field emission properties of vertically aligned double-walled carbon nanotube arrays. *Nanotechnology* **2008**, *19*, 415703, <https://doi.org/10.1088/0957-4484/19/41/415703>. 782-783
36. Izadi-Najafabadi, A.; Yamada, T.; Futaba, D.N.; Yudasaka, M.; Takagi, H.; Hatori, H.; Iijima, S.; Hata, K. High-Power Supercapacitor Electrodes from Single-Walled Carbon Nanohorn/Nanotube Composite. *ACS Nano* **2011**, *5*, 811-819, <https://doi.org/10.1021/nn1017457>. 784-786
37. Yalovega, G.E.; Brzhezinskaya, M.; Dmitriev, V.O.; Shmatko, V.A.; Ershov, I.V.; Ulyankina, A.A.; Chernysheva, D.V.; Smirnova, N.V. Interfacial Interaction in MeO_x/MWNTs (Me-Cu, Ni) Nanostructures as Efficient Electrode Materials for High-Performance Supercapacitors. *Nanomaterials* **2024**, *14*, 947, <https://doi.org/10.3390/nano14110947>. 787-788

38. Züttel, A.; Sudan, P.; Mauron, P.; Kiyobayashi, T.; Emmenegger, C.; Schlapbach, L. Hydrogen storage in carbon nanostructures. *Int. J. Hydrogen Energy* **2002**, *27*, 203-212, [https://doi.org/10.1016/S0360-3199\(01\)00108-2](https://doi.org/10.1016/S0360-3199(01)00108-2). 790-791
39. Brzhezinskaya, M.; Belenkov, E.A.; Greshnyakov, V.A.; Yalovega, G.E.; Bashkin, I.O. New aspects in the study of carbon-hydrogen interaction in hydrogenated carbon nanotubes for energy storage applications. *J. Alloys Compd.* **2019**, *792*, 713-720, <https://doi.org/10.1016/j.jallcom.2019.04.107>. 792-794
40. Landi, B.J.; Ganter, M.J.; Cress, C.D.; DiLeo, R.A.; Raffaele, R.P. Carbon nanotubes for lithium ion batteries. *Energy & Environmental Science* **2009**, *2*, 638-654, <https://doi.org/10.1039/b904116h>. 795-796
41. Lahiri, I.; Oh, S.W.; Hwang, J.Y.; Cho, S.; Sun, Y.K.; Banerjee, R.; Choi, W. High Capacity and Excellent Stability of Lithium Ion Battery Anode Using Interface-Controlled Binder-Free Multiwall Carbon Nanotubes Grown on Copper. *ACS Nano* **2010**, *4*, 3440-3446, <https://doi.org/10.1021/Nn100400r>. 797-799
42. Chen, G.H.; Dodson, B.; Hedges, D.M.; Steffensen, S.C.; Harb, J.N.; Puleo, C.; Galligan, C.; Ashe, J.; Vanfleet, R.R.; Davis, R.C. Fabrication of High Aspect Ratio Millimeter-Tall Free-Standing Carbon Nanotube-Based Microelectrode Arrays. *ACS Biomater. Sci. Eng.* **2018**, *4*, 1900-1907, <https://doi.org/10.1021/acsbiomaterials.8b00038>. 800-802
43. Yang, N.; Chen, X.P.; Ren, T.L.; Zhang, P.; Yang, D.G. Carbon nanotube based biosensors. *Sensor Actuat B-Chem* **2015**, *207*, 690-715, <https://doi.org/10.1016/j.snb.2014.10.040>. 803-804
44. Zhang, W.X.; Zhang, Z.Z.; Zhang, Y.G. The application of carbon nanotubes in target drug delivery systems for cancer therapies. *Nanoscale Res. Lett.* **2011**, *6*, 555, <https://doi.org/10.1186/1556-276x-6-555>. 805-806
45. Chen, G.H.; Sundaram, R.; Sekiguchi, A.; Hata, K.; Futaba, D.N. Through-Silicon-Via Interposers with Cu-Level Electrical Conductivity and Si-Level Thermal Expansion Based on Carbon Nanotube-Cu Composites for Microelectronic Packaging Applications. *ACS Appl. Nano Mater.* **2021**, *4*, 869-876, <https://doi.org/10.1021/acsnm.0c03278>. 807-809
46. Xu, M.; Du, F.; Ganguli, S.; Roy, A.; Dai, L.M. Carbon nanotube dry adhesives with temperature-enhanced adhesion over a large temperature range. *Nat. Commun.* **2016**, *7*, 13450, <https://doi.org/10.1038/ncomms13450>. 810-811
47. Qu, L.T.; Dai, L.M.; Stone, M.; Xia, Z.H.; Wang, Z.L. Carbon nanotube arrays with strong shear binding-on and easy normal lifting-off. *Science* **2008**, *322*, 238-242, <https://doi.org/10.1126/science.1159503>. 812-813
48. Chen, G.H.; Futaba, D.N.; Kimura, H.; Sakurai, S.; Yumura, M.; Hata, K. Absence of an Ideal Single-Walled Carbon Nanotube Forest Structure for Thermal and Electrical Conductivities. *ACS Nano* **2013**, *7*, 10218-10224, <https://doi.org/10.1021/nn404504f>. 814-815
49. Shibuya, A.; Chen, G.H.; Miyoshi, A.; Futaba, D.N. Improving the synthetic efficiency of single-wall carbon nanotube forests using a gas-analysis-designed mixed carbon feedstock. *Carbon* **2020**, *170*, 59-65, <https://doi.org/10.1016/j.carbon.2020.08.001>. 816-817
50. Chen, G.H.; Tsuji, T.; Yamada, M.; He, J.; Shimizu, Y.; Sakakita, H.; Hata, K.; Futaba, D.N.; Sakurai, S. Multi-step chemical vapor synthesis reactor based on a microplasma for structure-controlled synthesis of single-walled carbon nanotubes. *Chem. Eng. J.* **2022**, *444*, 136634, <https://doi.org/10.1016/j.cej.2022.136634>. 818-820
51. Sharma, P.; Pavelyev, V.; Kumar, S.; Mishra, P.; Islam, S.S.; Tripathi, N. Analysis on the synthesis of vertically aligned carbon nanotubes: growth mechanism and techniques. *J Mater Sci-Mater El* **2020**, *31*, 4399-4443, <https://doi.org/10.1007/s10854-020-03021-6>. 821-823
52. Chen, G.H.; Davis, R.C.; Futaba, D.N.; Sakurai, S.; Kobashi, K.; Yumura, M.; Hata, K. A sweet spot for highly efficient growth of vertically aligned single-walled carbon nanotube forests enabling their unique structures and properties. *Nanoscale* **2016**, *8*, 162-171, <https://doi.org/10.1039/C5NR05537G>. 824-826
53. Sugime, H.; Sato, T.; Nakagawa, R.; Hayashi, T.; Inoue, Y.; Noda, S. Ultra-long carbon nanotube forest via in situ supplements of iron and aluminum vapor sources. *Carbon* **2021**, *172*, 772-780, <https://doi.org/10.1016/j.carbon.2020.10.066>. 827-828
54. Lee, S.H.; Park, J.; Park, J.H.; Lee, D.M.; Lee, A.; Moon, S.Y.; Lee, S.Y.; Jeong, H.S.; Kim, S.M. Deep-injection floating-catalyst chemical vapor deposition to continuously synthesize carbon nanotubes with high aspect ratio and high crystallinity. *Carbon* **2021**, *173*, 901-909, <https://doi.org/10.1016/j.carbon.2020.11.065>. 829-831
55. Chen, G.H.; Seki, Y.; Kimura, H.; Sakurai, S.; Yumura, M.; Hata, K.; Futaba, D.N. Diameter control of single-walled carbon nanotube forests from 1.3-3.0 nm by arc plasma deposition. *Sci. Rep.* **2014**, *4*, 3804, <https://doi.org/10.1038/srep03804>. 832-833
56. Zhao, B.; Futaba, D.N.; Yasuda, S.; Akoshima, M.; Yamada, T.; Hata, K. Exploring Advantages of Diverse Carbon Nanotube Forests With Tailored Structures Synthesized by Supergrowth from Engineered Catalysts. *ACS Nano* **2009**, *3*, 108-114, <https://doi.org/10.1021/Nn800648a>. 834-836
57. Hiraoka, T.; Izadi-Najafabadi, A.; Yamada, T.; Futaba, D.N.; Yasuda, S.; Tanaike, O.; Hatori, H.; Yumura, M.; Iijima, S.; Hata, K. Compact and Light Supercapacitor Electrodes from a Surface-Only Solid by Opened Carbon Nanotubes with 2200 m² g⁻¹ Surface Area. *Adv. Funct. Mater.* **2010**, *20*, 422-428, <https://doi.org/10.1002/adfm.200901927>. 837-839
58. Xu, M.; Futaba, D.N.; Yumura, M.; Hata, K. Alignment Control of Carbon Nanotube Forest from Random to Nearly Perfectly Aligned by Utilizing the Crowding Effect. *ACS Nano* **2012**, *6*, 5837-5844, <https://doi.org/10.1021/nn300142j>. 840-841
59. Ci, L.; Vajtai, R.; Ajayan, P.M. Vertically aligned large-diameter double-walled carbon nanotube arrays having ultralow density. *J. Phys. Chem. C* **2007**, *111*, 9077-9080, <https://doi.org/10.1021/jp072123c>. 842-843
60. Tang, B.J.; Lu, Y.H.; Zhou, J.D.; Chouhan, T.; Wang, H.; Golani, P.; Xu, M.Z.; Xu, Q.; Guan, C.T.; Liu, Z. Machine learning-guided synthesis of advanced inorganic materials. *Mater Today* **2020**, *41*, 72-80, <https://doi.org/10.1016/j.mattod.2020.06.010>. 844-845

61. Yuan, R.H.; Liu, Z.; Balachandran, P.V.; Xue, D.Q.; Zhou, Y.M.; Ding, X.D.; Sun, J.; Xue, D.Z.; Lookman, T. Accelerated Discovery of Large Electrostrains in BaTiO₃-Based Piezoelectrics Using Active Learning. *Adv. Mater.* **2018**, *30*, 1702884, <https://doi.org/10.1002/adma.201702884>. 846
62. Lu, S.H.; Zhou, Q.H.; Ouyang, Y.X.; Guo, Y.L.; Li, Q.; Wang, J.L. Accelerated discovery of stable lead-free hybrid organic-inorganic perovskites via machine learning. *Nat. Commun.* **2018**, *9*, 3405, <https://doi.org/10.1038/s41467-018-05761-w>. 847
63. Xue, D.Z.; Balachandran, P.V.; Hogden, J.; Theiler, J.; Xue, D.Q.; Lookman, T. Accelerated search for materials with targeted properties by adaptive design. *Nat. Commun.* **2016**, *7*, 11241, <https://doi.org/10.1038/ncomms11241>. 848
64. Kaushal, A.; Alexander, R.; Rao, P.T.; Prakash, J.; Dasgupta, K. Artificial neural network, Pareto optimization, and Taguchi analysis for the synthesis of single-walled carbon nanotubes. *Carbon Trends* **2021**, *2*, 100016, <https://doi.org/10.1016/j.cartre.2020.100016>. 849
65. Shields, B.J.; Stevens, J.; Li, J.; Parasram, M.; Damani, F.; Alvarado, J.I.M.; Janey, J.M.; Adams, R.P.; Doyle, A.G. Bayesian reaction optimization as a tool for chemical synthesis. *Nature* **2021**, *590*, 89-96, <https://doi.org/10.1038/s41586-021-03213-y>. 850
66. Chu, D.M.; Ji, Z.C.; Zhang, X.J.; Zhao, X.Y.; He, Y.; Bai, W.J. Machine learning for the regulation strategy and mechanism of the integrated growth of carbon nanotube arrays. *New J. Chem.* **2023**, *47*, 21883-21896, <https://doi.org/10.1039/d3nj04124g>. 851
67. Bulmer, J.S.; Sloan, A.W.N.; Glerum, M.; Carpena-Nunez, J.; Waelder, R.; Humes, J.; Boies, A.M.; Pasquali, M.; Rao, R.; Maruyama, B. Forecasting carbon nanotube diameter in floating catalyst chemical vapor deposition. *Carbon* **2023**, *201*, 719-733, <https://doi.org/10.1016/j.carbon.2022.08.001>. 852
68. Ji, Z.H.; Zhang, L.L.; Tang, D.M.; Chen, C.M.; Nordling, T.E.M.; Zhang, Z.D.; Ren, C.L.; Da, B.; Li, X.; Guo, S.Y.; Liu, C.; Cheng, H.M. High-throughput screening and machine learning for the efficient growth of high-quality single-wall carbon nanotubes. *Nano Res.* **2021**, *14*, 4610-4615, <https://doi.org/10.1007/s12274-021-3387-y>. 853
69. Krasnikov, D.V.; Khabushev, E.M.; Gaev, A.; Bogdanova, A.R.; Iakovlev, V.Y.; Lantsberg, A.; Kallio, T.; Nasibulin, A.G. Machine learning methods for aerosol synthesis of single-walled carbon nanotubes. *Carbon* **2023**, *202*, 76-82, <https://doi.org/10.1016/j.carbon.2022.10.044>. 854
70. Shin, S.; Song, H.; Shin, Y.S.; Lee, J.; Seo, T.H. Bayesian Optimization of Wet-Impregnated Co-Mo/Al₂O₃ Catalyst for Maximizing the Yield of Carbon Nanotube Synthesis. *Nanomaterials* **2024**, *14*, 75, <https://doi.org/10.3390/nano14010075>. 855
71. Ding, R.; Chen, J.; Chen, Y.; Liu, J.; Bando, Y.; Wang, X. Unlocking the potential: machine learning applications in electrocatalyst design for electrochemical hydrogen energy transformation. *Chem. Soc. Rev.* **2024**, <https://doi.org/10.1039/D4CS00844H>. 856
72. Alwosheel, A.; van Cranenburgh, S.; Chorus, C.G. Is your dataset big enough? Sample size requirements when using artificial neural networks for discrete choice analysis. *Journal of Choice Modelling* **2018**, *28*, 167-182, <https://doi.org/10.1016/j.jocm.2018.07.002>. 857
73. Nikolaev, P.; Hooper, D.; Perea-Lopez, N.; Terrones, M.; Maruyama, B. Discovery of Wall-Selective Carbon Nanotube Growth Conditions via Automated Experimentation. *ACS Nano* **2014**, *8*, 10214-10222, <https://doi.org/10.1021/nn503347a>. 858
74. Nikolaev, P.; Hooper, D.; Webber, F.; Rao, R.; Decker, K.; Krein, M.; Poleski, J.; Barto, R.; Maruyama, B. Autonomy in materials research: a case study in carbon nanotube growth. *npj Comput Mater* **2016**, *2*, 16031, <https://doi.org/10.1038/npjcompumats.2016.31>. 859
75. Chang, J.; Nikolaev, P.; Carpena-Nunez, J.; Rao, R.; Decker, K.; Islam, A.E.; Kim, J.; Pitt, M.A.; Myung, J.I.; Maruyama, B. Efficient Closed-loop Maximization of Carbon Nanotube Growth Rate using Bayesian Optimization. *Sci. Rep.* **2020**, *10*, 9040, <https://doi.org/10.1038/s41598-020-64397-3>. 860
76. Li, Y.; Wang, S.; Lv, Z.; Wang, Z.; Zhao, Y.; Xie, Y.; Xu, Y.; Qian, L.; Yang, Y.; Zhao, Z. Transforming the Synthesis of Carbon Nanotubes with Machine Learning Models and Automation. *arXiv preprint arXiv:2404.01006* **2024**, <https://doi.org/10.48550/arXiv.2404.01006>. 861
77. Iijima, S. Helical Microtubules of Graphitic Carbon. *Nature* **1991**, *354*, 56-58, <https://doi.org/10.1038/354056a0>. 862
78. Qin, L.C. Electron diffraction from carbon nanotubes. *Rep Prog Phys* **2006**, *69*, 2761-2821, <https://doi.org/10.1088/0034-4885/69/10/R02>. 863
79. Jorio, A.; Saito, R.; Hafner, J.H.; Lieber, C.M.; Hunter, M.; McClure, T.; Dresselhaus, G.; Dresselhaus, M.S. Structural (n, m) determination of isolated single-wall carbon nanotubes by resonant Raman scattering. *Phys. Rev. Lett.* **2001**, *86*, 1118-1121, <https://doi.org/10.1103/PhysRevLett.86.1118>. 864
80. Dresselhaus, M.S.; Dresselhaus, G.; Saito, R.; Jorio, A. Raman spectroscopy of carbon nanotubes. *Phys. Rep.* **2005**, *409*, 47-99, <https://doi.org/10.1016/j.physrep.2004.10.006>. 865
81. Belianinov, A.; Vasudevan, R.; Strelcov, E.; Steed, C.; Yang, S.M.; Tselev, A.; Jesse, S.; Biegalski, M.; Shipman, G.; Symons, C.; Borisevich, A.; Archibald, R.; Kalinin, S. Big data and deep data in scanning and electron microscopies: deriving functionality from multidimensional data sets. *Advanced Structural and Chemical Imaging* **2015**, *1*, 6, <https://doi.org/10.1186/s40679-015-0006-6>. 866
82. Aguiar, J.A.; Gong, M.L.; Unocic, R.R.; Tasdizen, T.; Miller, B.D. Decoding crystallography from high-resolution electron imaging and diffraction datasets with deep learning. *Sci Adv* **2019**, *5*, eaaw1949, <https://doi.org/10.1126/sciadv.aaw1949>. 867
83. Cui, A.Y.; Jiang, K.; Jiang, M.H.; Shang, L.Y.; Zhu, L.Q.; Hu, Z.G.; Xu, G.S.; Chu, J.H. Decoding Phases of Matter by Machine-Learning Raman Spectroscopy. *Phys Rev Appl* **2019**, *12*, 054049, <https://doi.org/10.1103/PhysRevApplied.12.054049>. 868

84. Trejo, O.; Dadlani, A.L.; De La Paz, F.; Acharya, S.; Kravec, R.; Nordlund, D.; Sarangi, R.; Prinz, F.B.; Torgersen, J.; Dasgupta, N.P. Elucidating the Evolving Atomic Structure in Atomic Layer Deposition Reactions with in Situ XANES and Machine Learning. *Chem. Mater.* **2019**, *31*, 8937-8947, <https://doi.org/10.1021/acs.chemmater.9b03025>. 902-904
85. Kaufmann, K.; Zhu, C.Y.; Rosengarten, A.S.; Maryanovsky, D.; Harrington, T.J.; Marin, E.; Vecchio, K.S. Crystal symmetry determination in electron diffraction using machine learning. *Science* **2020**, *367*, 564-568, <https://doi.org/10.1126/science.aay3062>. 905-906
86. Spurgeon, S.R.; Ophus, C.; Jones, L.; Petford-Long, A.; Kalinin, S.V.; Olszta, M.J.; Dunin-Borkowski, R.E.; Salmon, N.; Hattar, K.; Yang, W.C.D.; Sharma, R.; Du, Y.G.; Chiamonti, A.; Zheng, H.M.; Buck, E.C.; Kovarik, L.; Penn, R.L.; Li, D.S.; Zhang, X.; Murayama, M.; Taheri, M.L. Towards data-driven next-generation transmission electron microscopy. *Nat. Mater.* **2021**, *20*, 274-279, <https://doi.org/10.1038/s41563-020-00833-z>. 907-910
87. Uchida, T.; Tazawa, M.; Sakai, H.; Yamazaki, A.; Kobayashi, Y. Radial breathing modes of single-walled carbon nanotubes in resonance Raman spectra at high temperature and their chiral index assignment. *Appl. Surf. Sci.* **2008**, *254*, 7591-7595, <https://doi.org/10.1016/j.apsusc.2008.01.107>. 911-913
88. Zhang, J.; Perrin, M.L.; Barba, L.; Overbeck, J.; Jung, S.; Grassy, B.; Agal, A.; Muff, R.; Brönnimann, R.; Haluska, M.; Roman, C.; Hierold, C.; Jaggi, M.; Calame, M. High-speed identification of suspended carbon nanotubes using Raman spectroscopy and deep learning. *Microsyst Nanoeng* **2022**, *8*, 19, <https://doi.org/10.1038/s41378-022-00350-w>. 914-916
89. Kajendarajah, U.; Avilés, M.O.; Lagugné-Labarthe, F. Deciphering tip-enhanced Raman imaging of carbon nanotubes with deep learning neural networks. *Phys. Chem. Chem. Phys.* **2020**, *22*, 17857-17866, <https://doi.org/10.1039/d0cp02950e>. 917-918
90. Luo, Q.X.; Holm, E.A.; Wang, C. A transfer learning approach for improved classification of carbon nanomaterials from TEM images. *Nanoscale Adv* **2021**, *3*, 206-213, <https://doi.org/10.1039/d0na00634c>. 919-920
91. Kalinin, S.V.; Ziatdinov, M.; Spurgeon, S.R.; Ophus, C.; Stach, E.A.; Susi, T.; Agar, J.; Randall, J. Deep learning for electron and scanning probe microscopy: From materials design to atomic fabrication. *MRS Bull.* **2022**, *47*, 931-939, <https://doi.org/10.1557/s43577-022-00413-3>. 921-923
92. Govind, K.; Oliveros, D.; Dlouhy, A.; Legros, M.; Sandfeld, S. Deep learning of crystalline defects from TEM images: a solution for the problem of 'never enough training data'. *Mach Learn-Sci Techn* **2024**, *5*, 015006, <https://doi.org/10.1088/2632-2153/ad1a4e>. 924-925
93. Förster, G.D.; Castan, A.; Loiseau, A.; Nelayah, J.; Alloyeau, D.; Fossard, F.; Bichara, C.; Amara, H. A deep learning approach for determining the chiral indices of carbon nanotubes from high-resolution transmission electron microscopy images. *Carbon* **2020**, *169*, 465-474, <https://doi.org/10.1016/j.carbon.2020.06.086>. 926-928
94. Lee, B.; Yoon, S.; Lee, J.W.; Kim, Y.; Chang, J.; Yun, J.; Ro, J.C.; Lee, J.S.; Lee, J.H. Statistical Characterization of the Morphologies of Nanoparticles through Machine Learning Based Electron Microscopy Image Analysis. *ACS Nano* **2020**, *14*, 17125-17133, <https://doi.org/10.1021/acsnano.0c06809>. 929-931
95. Chen, D.; Gao, J.; He, D.; He, J.; Li, Y.; Zhang, M.; Li, W.; Chen, X.; He, X.; Fu, T. Plasmonic Bridge Sensor Enabled by Carbon Nanotubes and Au-Ag Nano-Rambutan for Multifunctional Detection of Biomechanics and Bio/Chemical Molecules. *ACS Appl. Mater. Interfaces* **2023**, *15*, 8783-8793, <https://doi.org/10.1021/acsnano.2c22634>. 932-934
96. Kelich, P.; Adams, J.; Jeong, S.; Navarro, N.; Landry, M.P.; Vukovic, L. Predicting Serotonin Detection with DNA-Carbon Nanotube Sensors across Multiple Spectral Wavelengths. *J. Chem. Inf. Model.* **2024**, *64*, 3992-4001, <https://doi.org/10.1021/acs.jcim.4c00021>. 935-937
97. Tadokoro, Y.; Funayama, K.; Kawano, K.; Miura, A.; Hirotsu, J.; Ohno, Y.; Tanaka, H. Artificial-intelligence-assisted mass fabrication of nanocantilevers from randomly positioned single carbon nanotubes. *Microsyst Nanoeng* **2023**, *9*, 32, <https://doi.org/10.1038/s41378-023-00507-1>. 938-940
98. Aliyana, A.K.; Kumar, S.K.N.; Marimuthu, P.; Baburaj, A.; Adetunji, M.; Frederick, T.; Sekhar, P.; Fernandez, R.E. Machine learning-assisted ammonium detection using zinc oxide/multi-walled carbon nanotube composite based impedance sensors. *Sci. Rep.* **2021**, *11*, 24321, <https://doi.org/10.1038/s41598-021-03674-1>. 941-943
99. Bian, L.; Wang, Z.H.; White, D.L.; Star, A. Machine learning-assisted calibration of Hg²⁺ sensors based on carbon nanotube field-effect transistors. *Biosens. Bioelectron.* **2021**, *180*, 113085, <https://doi.org/10.1016/j.bios.2021.113085>. 944-945
100. Fan, G.; Low, K.L. Physics-Integrated Machine Learning for Efficient Design and Optimization of a Nanoscale Carbon Nanotube Field-Effect Transistor. *ECS Journal of Solid State Science and Technology* **2023**, *12*, 091005, <https://doi.org/10.1149/2162-8777/acfb38>. 946-947
101. Kelich, P.; Jeong, S.; Navarro, N.; Adams, J.; Sun, X.Q.; Zhao, H.H.; Landry, M.P.; Vukovic, L. Discovery of DNA-Carbon Nanotube Sensors for Serotonin with Machine Learning and Near-infrared Fluorescence Spectroscopy. *ACS Nano* **2022**, *16*, 736-745, <https://doi.org/10.1021/acsnano.1c08271>. 948-950
102. Yu, T.Y.; Mo, X.D.; Chen, M.J.; Yao, C.F. Machine-learning-assisted microstructure-property linkages of carbon nanotube-reinforced aluminum matrix nanocomposites produced by laser powder bed fusion. *Nanotechnol Rev* **2021**, *10*, 1410-1424, <https://doi.org/10.1515/ntrev-2021-0093>. 951-953
103. Ranaiefar, M.; Singh, M.; Halbig, M.C. Additively Manufactured Carbon-Reinforced ABS Honeycomb Composite Structures and Property Prediction by Machine Learning. *Molecules* **2024**, *29*, 2736, <https://doi.org/10.3390/molecules29122736>. 954-955
104. Jalal, M.; Moradi-Dastjerdi, R.; Bidram, M. Big data in nanocomposites: ONN approach and mesh-free method for functionally graded carbon nanotube-reinforced composites. *J Comput Des Eng* **2019**, *6*, 209-223, <https://doi.org/10.1016/j.jcde.2018.05.003>. 956-957

105. Huang, J.S.; Liew, J.X.; Liew, K.M. Data-driven machine learning approach for exploring and assessing mechanical properties of carbon nanotube-reinforced cement composites. *Compos Struct* **2021**, *267*, 113917, <https://doi.org/10.1016/j.compstruct.2021.113917>. 958
959
960
106. Bagherzadeh, F.; Shafighard, T. Ensemble Machine Learning approach for evaluating the material characterization of carbon nanotube-reinforced cementitious composites. *Case Stud Constr Mat* **2022**, *17*, e01537, <https://doi.org/10.1016/j.cscm.2022.e01537>. 961
962
107. Okasha, N.M.; Mirrashid, M.; Naderpour, H.; Ciftcioglu, A.O.; Meddage, D.P.P.; Ezami, N. Machine learning approach to predict the mechanical properties of cementitious materials containing carbon nanotubes. *Developments in the Built Environment* **2024**, *19*, 100494, <https://doi.org/10.1016/j.dibe.2024.100494>. 963
964
965
108. Le, T.-T. Prediction of tensile strength of polymer carbon nanotube composites using practical machine learning method. *J. Compos Mater.* **2021**, *55*, 787-811, <https://doi.org/10.1177/0021998320953540>. 966
967
109. Liu, B.K.; Vu-Bac, N.; Zhuang, X.Y.; Fu, X.L.; Rabczuk, T. Stochastic integrated machine learning based multiscale approach for the prediction of the thermal conductivity in carbon nanotube reinforced polymeric composites. *Compos. Sci. Technol.* **2022**, *224*, 109425, <https://doi.org/10.1016/j.compscitech.2022.109425>. 968
969
970
110. Liu, B.K.; Vu-Bac, N.; Zhuang, X.Y.; Fu, X.L.; Rabczuk, T. Stochastic full-range multiscale modeling of thermal conductivity of Polymeric carbon nanotubes composites: A machine learning approach. *Compos Struct* **2022**, *289*, 115393, <https://doi.org/10.1016/j.compstruct.2022.115393>. 971
972
973
111. Champa-Bujaico, E.; Díez-Pascual, A.M.; Garcia-Diaz, P.; Sessini, V.; Mosquera, M.E.G. Machine learning algorithms to optimize the properties of bio-based poly (butylene succinate-co- butylene adipate) nanocomposites with carbon nanotubes. *Ind Crop Prod* **2024**, *219*, 119018, <https://doi.org/10.1016/j.indcrop.2024.119018>. 974
975
976
112. Zarei, A.; Farazin, A. Machine Learning Insights into the Influence of Carbon Nanotube Dimensions on Nanocomposite Properties: A Comprehensive Exploration. *Journal of Computational Applied Mechanics* **2024**, *55*, 462-472, <https://doi.org/10.22059/jcamech.2024.376321.1086>. 977
978
979
113. Chen, G.H.; Dodson, B.; Johnson, F.; Hancu, I.; Fiveland, E.; Zhang, W.; Galligan, C.; Puleo, C.; Davis, R.C.; Ashe, J.; Vanfleet, R.R. Tissue-susceptibility matched carbon nanotube electrodes for magnetic resonance imaging. *J. Magn. Reson.* **2018**, *295*, 72-79, <https://doi.org/10.1016/j.jmr.2018.08.003>. 980
981
982
114. Ouassil, N.; Pinals, R.L.; Del Bonis-O'Donnell, J.T.; Wang, J.W.; Landry, M.P. Supervised learning model predicts protein adsorption to carbon nanotubes. *Sci Adv* **2022**, *8*, eabm0898, <https://doi.org/10.1126/sciadv.abm0898>. 983
984
115. Lee, D.; Lee, J.; Kim, W.; Suh, Y.; Park, J.; Kim, S.; Kim, Y.; Kwon, S.; Jeong, S. Systematic Selection of High-Affinity ssDNA Sequences to Carbon Nanotubes. *Adv Sci* **2024**, *11*, 2308915, <https://doi.org/10.1002/advs.202308915>. 985
986
116. Lin, Z.W.; Yang, Y.; Jagota, A.; Zheng, M. Machine Learning-Guided Systematic Search of DNA Sequences for Sorting Carbon Nanotubes. *ACS Nano* **2022**, *16*, 4705-4713, <https://doi.org/10.1021/acsnano.1c11448>. 987
988
117. Kotzabasaki, M.; Sotiropoulos, I.; Charitidis, C.; Sarimveis, H. Machine learning methods for multi-walled carbon nanotubes (MWCNT) genotoxicity prediction. *Nanoscale Adv* **2021**, *3*, 3167-3176, <https://doi.org/10.1039/d0na00600a>. 989
990
118. Gong, X.; Renegar, N.; Levi, R.; Strano, M.S. Machine learning for the discovery of molecular recognition based on single-walled carbon nanotube corona-phases. *npj Comput Mater* **2022**, *8*, 135, <https://doi.org/10.1038/s41524-022-00795-7>. 991
992
993
994

Disclaimer/Publisher's Note: The statements, opinions and data contained in all publications are solely those of the individual author(s) and contributor(s) and not of MDPI and/or the editor(s). MDPI and/or the editor(s) disclaim responsibility for any injury to people or property resulting from any ideas, methods, instructions or products referred to in the content. 995
996
997
998